

1 **TiO₂/Cu(II) photocatalytic production of benzaldehyde from benzyl**
2 **alcohol in solar pilot plant reactor**

3 Danilo Spasiano^{a*}, Lucia del Pilar Prieto Rodriguez^b, Jaime Carbajo Olleros^c, Sixto Malato^b,
4 Raffaele Marotta^a, Roberto Andreozzi^a

5
6 ^a **Dipartimento di Ingegneria Chimica, dei Materiali e della Produzione Industriale**, Università
7 di Napoli “Federico II”, p.le V. Tecchio, 80 – 80125 – Naples, Italy.

8 ^b Plataforma Solar de Almería-CIEMAT, Carretera de Senés Km 4 - 04200 - Tabernas, Almería,
9 Spain.

10 ^c Departamento de Ingeniería de Procesos Catalíticos Instituto de Catálisis y Petroleoquímica, CSIC,
11 C/ Marie Curie 2 - 28049 - Cantoblanco, Madrid, Spain.

12
13 * Corresponding author. Tel +390817682968 fax +390815936936. E-mail danilo.spasiano@unina.it

14
15 **ABSTRACT**

16 The technical feasibility of selective photocatalytic oxidation of benzyl alcohol to benzaldehyde, in
17 aqueous solutions, in presence of cupric ions has been investigated in a solar pilot plant with
18 Compound Parabolic Collectors. Aldrich (pure anatase) and P25 Degussa TiO₂ have been used as
19 photocatalysts. The influences of cupric species concentrations, solar irradiance and temperature are
20 discussed too. The oxidation rates were strongly influenced by the initial cupric ions concentration,
21 incident solar irradiance and temperatures.

22 The best results found, in terms of yields and selectivities to benzaldehyde under acidic conditions
23 were higher than 50% and 60% respectively under acidic conditions.

1 Under deaerated conditions, the presence of reduced copper species was proved by XPS analysis.
2 The results indicated that, at the end of the process, cupric species can be easily regenerated and
3 reused, through a re-oxidation of reduced copper, produced during the photolytic run, with air or
4 oxygen in dark conditions.

5 A figure-of-merit (A_{CM}), proposed by the International Union of Pure and Applied Chemistry
6 (IUPAC) and based on the collector area, has been estimated, under the proposed conditions, with
7 the aim to provide a direct link to the solar-energy efficiency independently of the nature of the
8 system. Generally speaking, it can be considered that **the** lower A_{CM} values **the** higher the system
9 efficiency.

10

11 *Keywords:* selective oxidation, benzyl alcohol, benzaldehyde production, TiO₂ photocatalysis, solar
12 photocatalytic plant, figure-of-merit.

13

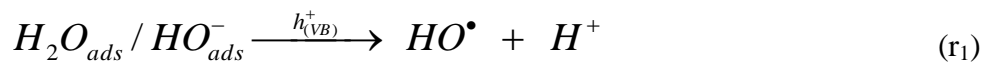
14 **1. Introduction**

15 The use of TiO₂, as readily available and environmentally friendly photocatalyst, was largely
16 investigated for the removal of non-biodegradable or undesirable organic substances from
17 wastewater [1-3] and TiO₂ based on solar technologies were developed during the past years for
18 reducing the cost of large-scale aqueous-phase applications to treat industrial wastewater [4,5].
19 However, only in recent years the research has pointed its attention on the possibility to use the
20 TiO₂ as a photocatalyst for the selective oxidation of organic molecules under UV radiation in non
21 aqueous media [6]. For example, the selective oxidation of aromatic alcohols in the respective
22 aldehydes can be easily gained in acetonitrile or in solvent free systems at room temperature [7,8]
23 due to the reaction of the alcoholic substrate with the photogenerated positive holes (h_{vb}^+) and using
24 oxygen as acceptor of photoelectrons [9]. In particular, the addition of an organic solvent, as
25 acetonitrile, allows the oxidation of benzyl alcohol and its derivatives with selectivities to the

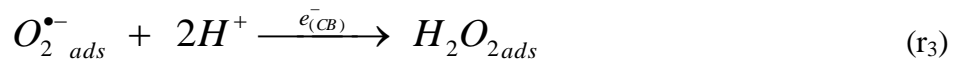
1 respective aldehydes of over 90% [8,10], values well higher than those reported (10-60%) when the
2 same process is carried out in aqueous solutions using TiO₂ nanoparticles [11,12].

3 Moreover, selectivities of 41-74% were reported for the oxidation of 4-substituted aromatic
4 alcohols to the corresponding aldehydes, using aqueous media, over rutile or anatase TiO₂ catalysts
5 [11,13]. The decrease of the selectivity in aqueous solution with respect the use of organic non
6 aqueous solvent is mainly due to [9]:

7 a) formation of very reactive species such as hydroxyl radicals (HO•) through the reaction of
8 adsorbed water molecules or hydroxyl groups with positive holes:

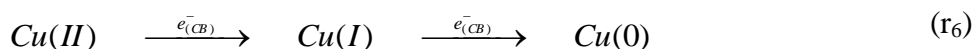


9 b) generation of radical superoxide (O₂^{•-}) by the reaction of molecular oxygen with photogenerated
10 electrons (r₂). **In presence of water, O₂^{•-} species gives rise to hydrogen peroxide (r₃)** whose
11 electron trapping generates HO• radicals (r₄), which oxidizes not selectively the organic substances
12 (r₅):



13 On the other side, water is considered the best solvent for environmental friendly process and, for
14 this reason, other new approaches have arisen in order to avoid the use the organic solvents. In
15 particular, very recent studies demonstrated that the use of Cu(II) ions, as electron acceptor, instead
16 of molecular oxygen, under deaerated conditions, leads to an increase of selectivity to benzaldehyde
17 up to 72%, starting from benzyl alcohol [14], since the formation of hydroxyl radicals takes place
18 just by the reaction of water molecules or surface adsorbed hydroxyl groups with positive holes. In

1 this case, cupric ions reduce to a lower state of oxidation by capturing the photogenerated electron
2 on the TiO₂ surface and precipitate from the solution:



3 whereas adsorbed benzyl alcohol (BA) is oxidized to the benzaldehyde (BHA), through a direct
4 reaction with the positive holes:



5 At the end of the process, cupric ions could be regenerated and reused, through the reoxidation of
6 zero valent precipitated copper with an air flow at dark conditions.

7 Chemical state of solid copper after the photocatalytic run was also intensively investigated, but
8 controversial results were reported. Most of the researchers reported that the solid is composed by a
9 mixture of zero valent copper and cupric oxide (and, in some case, cuprous oxide) [15-19].

10 In some studies it was concluded that the reduced Cu species was zero valent copper [20-21].
11 However, the possibility of the presence of both Cu(I)/Cu(II) species, due to a reoxidation of metal
12 copper during the preparation of the analytical samples, was not completely ruled out [22].

13 At best of the Authors' knowledge, only lab-scale lamp-driven investigations on the selective TiO₂
14 photocatalytic oxidation of benzyl alcohol and its derivatives, in aqueous or acetonitrile or solvent
15 free systems, were reported in the literature [11, 12, 14, 23-27].

16 It could be very interesting, for economic and environmental reasons, to evaluate the possibility of
17 exploiting the use of solar radiations **daily** arriving on the earth surface, through the use of pilot
18 plants, for the production of benzaldehyde from benzyl alcohol.

19 In the present work, the development of the TiO₂/Cu(II)/solar radiation system for the selective
20 oxidation of benzyl alcohol to benzaldehyde in water is studied, by using a solar photocatalytic pilot
21 plant at different operating conditions (TiO₂ photocatalyst type, Cu(II) initial concentration and
22 irradiance of solar radiation). The possibility of reuse copper as catalyst **is** also tested by oxidizing
23 the precipitated zero valent copper with an air flow blown into the pilot-plant in dark conditions.

1 Optimal conditions of TiO₂ load and pH values **are** fixed according to the ones found in previous
2 studies [14,28].

3 Moreover, analyses of solid, after the oxidation runs, **are** carried out to better clarify the nature of
4 copper species at the end of the process.

5

6 **2. Material and methods**

7 *2.1 Experimental set-up and procedures*

8 *2.1.1 Pilot-Plant experiments*

9 Experimental investigations were carried out, from May to July 2012, in a solar pilot-plant
10 consisting of twelve Compound Parabolic Collectors (CPC), installed in the Plataforma Solar de
11 Almería (37° latitude N, Spain) and elsewhere described in its geometrical and functional
12 characteristics [29]. The total solution volume is 39 l, where only 22 l are exposed to solar
13 radiation; the rest is distributed between the recirculation tank (9 l) and the hydraulic connections (8
14 l). The recirculation tank of the adopted CPC was modified, as reported in figure 1, in order to
15 ensure the absence of oxygen, essential for performing the proposed process. For this purpose, the
16 solutions, containing the catalysts and the substrate, were preventively purged with nitrogen
17 gaseous stream through two porous ceramic spargers, by closing the valve V_n, to remove the
18 dissolved oxygen. During the experimental runs a continuous nitrogen flow was guaranteed to the
19 reactor to prevent the entry of air in the reactor but it was switched in the freeboard of the
20 recirculation tank, by opening the valve V_n, to inhibit the stripping of organic substances from the
21 solution. In the last case, the bubbling of nitrogen is strongly limited by the pressure drop due to the
22 spargers.

23 To better follow the concentration profiles of the compounds involved in the process, some
24 experimental runs were carried out during two days. In these cases, **at the end of the first day**, the
25 irradiated part of the reactor was covered and the recycling tank was capped to stop the
26 photochemical reactions and to prevent the entry of oxygen respectively.

1 Samples were collected in a glass bottle at different reaction times, by opening the valve V_s , rapidly
2 filtered to prevent the reoxidation of precipitate copper and finally analyzed.

3 All the experimental data were reported in function of the accumulated energy, per unit of volume
4 (kJ/l), incident on the reactor at the corresponding time of the withdrawn sample (Q_n) [30]:

$$Q_n = Q_{n-1} + \Delta t_n \cdot \overline{UV}_n \cdot \frac{A_r}{V_t}; \quad \Delta t_n = t_n - t_{n-1} \quad (\text{eq. 1})$$

5 where Q_{n-1} represent the accumulated energy (per unit of volume, kJ/l) taken during the experiment
6 relative to the previous sampling; Δt_n , \overline{UV}_n and V_t are, respectively, the elapsed time, the average
7 UV-irradiance (measured by a global UV radiometer KIPP&ZONEN, model CUV 3 mounted on a
8 platform tilted the same angle as the CPCs) which reaches the collector surface (A_r) between the
9 two samplings and the total solution volume.

10

11 *2.1.2 Laboratory-scale experiments*

12 Experiments were carried out in a Suntest solar simulator (Suntest XLS+ photoreactor, Atlas)
13 equipped with a 765-250 W/m² Xenon lamp (61-24 W/m² from 300 nm to 400 nm, $1.4 \cdot 10^{20}$ -
14 $5.5 \cdot 10^{19}$ photons/m²·s) and a cooler to keep the temperature at 35°C. The UV irradiation, in the
15 range of 300-400 nm, was monitored by using a portable radiometer (Solar Light CO PMA 2100)
16 fixed on the shaker inside the lamp influence zone, like shown in figure 2.

17 In this case, a volume of 700 ml of reacting solution was prepared in a one liter flask and, after 30
18 minutes of stripping with nitrogen, was rapidly poured in ten cylindrical glass vials with the
19 capacity of 42 ml and a diameter of 25 mm. The vials were rapidly closed with a screw cap, to
20 prevent the entry of oxygen, and were simultaneously exposed to the lamp radiation and agitated by
21 a shaker like shown in figure 2. The temperature was set at 35 °C. Each vial represented a sample to
22 remove from the solar box at different reaction times. Once collected, all the samples were rapidly
23 filtered and analyzed.

1 The pH of the solutions was adjusted at the value of 2.0, for all the runs, by using an aqueous
2 solution of 85% of phosphoric acid.

3 *2.2 Analytical methods*

4 The concentrations of benzyl alcohol, benzaldehyde and benzoic acid at different reaction times
5 were evaluated by HPLC analysis. For this purpose, the HPLC apparatus (Agilent 1100) was
6 equipped with a diode array UV/Vis detector ($\lambda = 215, 230, 250$ nm) and Phenomenex (Gemini 5u
7 C18 150x3 mm) column, using a mobile phase flowing at 0.7 ml min^{-1} . The mobile phase was
8 prepared by a buffer solution (A), H₂O (B) and CH₃CN (C). A linear gradient progressed from 15%
9 C to 28% C and from 45% B to 32% B in 10 minutes with a subsequent re-equilibrium time of 3
10 minutes. One liter of buffer was made by 10 ml of phosphoric acid solution (5.05 M), 50 ml of
11 methyl alcohol and water for HPLC.

12 The concentration of dissolved copper ions was measured by means of a colorimetric method using
13 an analytical kit (based on oxalic acid bis-cyclohexylidene hydrazide, cuprizone®) purchased from
14 Macherey-Nagel. An UV/Vis spectrometer (UNICAM-II spectrophotometer) has been used for the
15 measurements at a wavelength of 585 nm.

16 Total organic carbon (TOC) was monitored by Shimadzu Total Organic Carbon analyser model
17 TOC-5050A, equipped with an auto sampler ASI 5000A. The pH was monitored by a portable pH-
18 meter (Crison pH 25).

19 The Cu/Ti ratio for unknown solids, withdrawn at the end of some photocatalytic runs, was
20 estimated by an Energy Dispersive X-ray spectrometer system (SwiftED, Oxford Instruments)
21 attached to a Scanning Electron Microscope (TM-1000, Hitachi).

22 Powder X-ray diffraction (XRD) patterns were estimated using a X'PertPRO (PANalytical)
23 diffractometer with nickel-filtered Cu K α radiation. The X-ray generator was operated at 45 kV and
24 40 mA. The powders were scanned from $2\theta = 4^\circ$ to 90° with a 0.02 step size and accumulating a
25 total of 5 s per point.

1 X-ray photoelectron spectroscopy (XPS) analysis was carried out under high vacuum chamber with
2 a base pressure below 9×10^{-7} Pa at room temperature. Photoemission spectra were recorded using a
3 SPECS GmbH system equipped with an UHV PHOIBOS 150 analyser with Al monochromatic
4 anode operated at 12 kV and 200 W with a photon energy of $h\nu = 1486.74$ eV. A pass energy of 25
5 eV was used for high-resolution scans. Binding energies (BE) were referenced to C1s peak (284.6
6 eV) to take into account charging effects.

7 The XPS spectra obtained were then curved fitted using the XPS PeakFit software. The areas of the
8 peaks were computed by fitting the experimental spectra to Gaussian/Lorentzian curves after
9 subtracting the background (Shirley function).

10

11 *2.3 Materials*

12 Two commercial microcrystalline TiO₂ powders were tested: TiO₂ Degussa P25 (80% anatase, 20%
13 rutile, BET specific surface area $50 \text{ m}^2 \text{ g}^{-1}$) and TiO₂ Aldrich (pure anatase phase, BET specific
14 surface area $9.5 \text{ m}^2 \text{ g}^{-1}$).

15 Cupric ions were introduced in the system as anhydrous cupric sulphate (Sigma-Aldrich) with a
16 purity >99.0% (w/w). Benzyl alcohol (BA), benzaldehyde (BHA) and benzoic acid (BAC), with a
17 purity >99.0% (w/w), were purchased from Sigma Aldrich and used as received. Phosphoric acid
18 with a purity 85% from Merck as used as received

19

20 **3. Result and discussion**

21 *3.1 Effect of TiO₂ type*

22 The results obtained during different experimental runs of solar photo-oxidation of benzyl alcohol,
23 with two different typologies of commercial TiO₂ samples, at the same load (200 mg/l), are shown
24 in figures 3a-b.

25 The runs were carried out in two days. At the end of first day, when the reactor was covered, the
26 UV-irradiances (wavelength 300-400 nm) and temperatures decreased (see figs 3a,b). During the

1 runs, measured UV-irradiances ranged between 40 and 50 W/m² approximately (fig. 3b,
2 **continuous and dashed lines**).

3 As shown in the diagrams, the reactivity of the system is higher when TiO₂ P25 by Degussa is used
4 than the TiO₂ Aldrich catalyst. In particular, in presence of P25 Degussa sample (empty symbols),
5 for a Q_n value of 123 kJ/l, the BA concentration approached to zero (figure 3a) and Cu(II) ions were
6 totally reduced (figure 3b), whereas, if Aldrich TiO₂ sample is used (full symbols), about 27% of
7 initial benzyl alcohol and Cu(II) ions were still present in the solution.

8 The higher reactivity observed for the system in presence of P25 Degussa TiO₂ is in disagreement
9 with the results, previously reported [14], that show a similar reactivity when P25 Degussa and
10 Aldrich TiO₂ catalysts were used in presence of an UV radiation emitted by a laboratory
11 thermostated lamp.

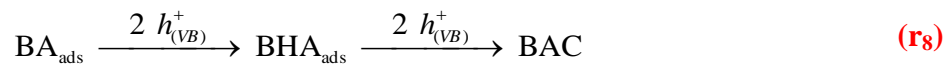
12 **This discrepancy may be probably due to the different emission spectra between lamp and the**
13 **sun and (different) light absorption characteristics, in the range of 300-800 nm, of the two**
14 **used catalysts.**

15 **Moreover, the different reactivities, recorded in the solar experiments, could be also**
16 **attributed to the differences between the averages of the measured temperatures: 38.6 °C and**
17 **34.3 °C for runs carried out in presence of Degussa P25 (dotted lines) and Aldrich TiO₂**
18 **(dashed and dotted lines) catalysts respectively (fig 3a).**

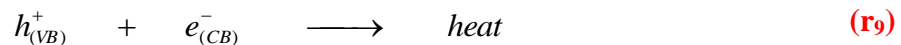
19 **As shown in figure 4**, the BA solar photocatalytic oxidation resulted in the production of BHA
20 **(diamonds)** for **Aldrich (full symbols)** and **P25 Degussa (empty symbols) TiO₂** catalysts, and
21 BAC an undesired product that derives from the reaction between the positive photogenerated holes
22 on the TiO₂ surface and benzaldehyde. BAC yields are also reported **in** the same figure **(triangles)**.

23 According to the previous results, the highest BHA production rates were gained in presence of P25
24 Degussa TiO₂. **Moreover, for this catalyst, the maximum BAC production rate was reached at**
25 **the highest yields of BHA.**

1 **However**, for accumulated energy values higher than 80 kJ/l, **when the unconverted BA**
2 **concentration was less than 20% of its initial concentration (fig. 3a, empty squares)**, a decrease
3 in BHA yield with respect of initial BA amount, from the value of 53.3% to 45.5%, was observed
4 using P25 Degussa TiO₂ samples. This result can be explained by considering a competition in the
5 reaction between the BA and BHA molecules **for** the photogenerated positive holes on the TiO₂:



6 **It is interesting to remark that for accumulated energy values higher than 120 kJ/l, in the case**
7 **of Degussa TiO₂ catalyst, when Cu(I)/Cu(II) species are totally reduced (fig. 3b, empty**
8 **squares), being the predominant reaction the recombination between photoinduced positive**
9 **holes and electrons:**



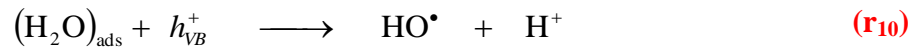
10 **the BA (fig. 3a, empty squares) and BHA (fig. 4, empty diamonds) consumption and BAC**
11 **production rates (fig. 4, empty triangles) stopped.**

12 The BHA selectivity, with respect to BA consumption, was calculated for both TiO₂ types (fig. 5).
13 As shown in the diagram, it seems that the use of Aldrich TiO₂ sample renders the system more
14 selective, reaching, for Q_n values of 130 kJ/l, BHA selectivity values close to 70% **(in presence of**
15 **P25 Degussa, only a value of 50% was obtained).**

16 **The highest selectivity achieved in presence of Aldrich TiO₂ sample is correlated at the lower**
17 **degree of conversion (fig. 3a, full squares) when compared with the test in which Degussa P25**
18 **is used (fig. 3a, empty squares)**

19 TOC measurements collected during the runs are also reported in figure 5, in terms of
20 mineralization degrees. **Due to the HO radicals generation from the reaction of water molecules**
21 **or surface adsorbed hydroxyl groups with positive holes [37]:**

22



1 the **two** trends are very similar, with a degree of mineralization at the end of the experimental runs
2 of 9% and 7% in presence of P25 Degussa and Aldrich TiO₂ respectively,

3 **However, the low degree of mineralization achieved demonstrates the possibility of using such**
4 **system to carry out selective oxidations in aqueous media.**

5

6 *3.2 Effect of cupric ions concentration*

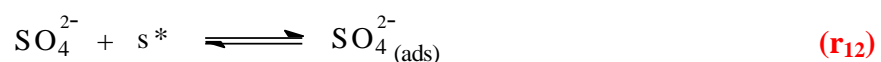
7 To evaluate the effect of Cu(II) initial concentration, some experimental runs of solar photooxidation
8 of benzyl alcohol were carried out with Aldrich TiO₂ at the load of 200 mg/l and pH = 2.0, varying
9 the cupric ions starting concentration (0.5 mM, 1.0 mM and 1.5 mM).

10 As shown in figures 6a-b, the temperatures and UV-irradiance profiles (solid, dashed and dotted
11 lines) are so similar as to be considered equals for the three runs.

12 With Cu(II) and BA starting concentrations of 0.5 mM and 1.5 mM **respectively**, the BA oxidation
13 stopped for Q_n values close to 35 kJ/l where a complete reduction of cupric ions was observed (full
14 triangles).

15 **At the highest Cu(II) initial concentration (1.5 mM), it** resulted into a decrease of the system
16 reactivity and BA conversion (fig. 6a, full circles) and, at the same time, the Cu(II) reduction rates
17 decrease. The observed results, according to those previously reported [14], are probably due to a
18 partial catalyst deactivation by the adsorbed sulphate ions which may block the TiO₂ active sites

19 **(s*)** [31]:



20 In fact, since Cu(II) species were **added** to the reactive solution as cupric sulphate (CuSO₄),
21 increasing the Cu(II) ions initial concentration results into an increase of sulphate concentration too.

1 Moreover, the sulphate anions, at concentration level higher than 1.0 mM, exerted a negative effect,
2 inhibiting the BA photo-oxidation rates because they are in competition with BA molecules in the
3 reaction with the positive holes [14]:



4 In figure 7 are reported the experimental concentration profiles of BHA and BAC (full and empty
5 symbols) that are in agreement with BA concentration trends shown in figure 6a. In particular the
6 best result found, in term of yield, was of 43% for BHA, starting with $[\text{Cu(II)}]_0 = 1.0 \text{ mM}$, for a
7 accumulated energy value of 67 kJ/l. For all the runs, the selectivity was always higher than 67%
8 and the mineralization degrees were lower than 4.5% (data not shown).

9

10 *3.3 Effect of the irradiance and temperature*

11 As previously shown in the figures 3b and 6b, the Cu(II) concentrations are characterized by a s-
12 shaped profile and, in particular, when the solar UV radiations and reactor temperatures reached the
13 top, a marked increase of Cu(II) reduction rate was observed. With the aim to better assess the
14 relationship between the variability of both irradiances and temperatures during a solar run and the
15 s-shaped of cupric ions concentration profile, a set of three laboratory photolytic experiments, with
16 Cu(II) initial concentration equal to 0.5 mM, were carried out at three different irradiances, kept
17 constant during a single run and under controlled solution temperature ($T=35 \text{ }^\circ\text{C}$). For this purpose,
18 a solar box apparatus, described in the experimental section, was used. Since the internal diameters
19 of CPC solar reactor tubes and the solar box vials are 31 mm and 24 mm respectively, the TiO_2 load
20 that maximizes the adsorption of UV radiation emitted by solar lamp is higher than **that** used for
21 solar experiments carried out in CPC reactor.

22 The optimum TiO_2 concentration (c_{cat}), for which the optical thickness equals that of CPC reactor
23 configuration ($\tau=9.12$) can be easily calculated as suggested by others [28,32]:

$$c_{cat} = \frac{\tau}{(\sigma + k) \times d} = 258 \text{ mg/l} \quad \text{eq. 2}$$

1 where σ is the scattering coefficient ($1.295 \cdot 10^3 \text{ m}^2/\text{kg}$), k is the catalyst specific mass absorption
 2 ($1.75 \cdot 10^2 \text{ m}^2/\text{kg}$) and d the internal tube diameter (24 mm).

3 As shown in figure 8, by increasing the UV irradiance from 39.5 W/m^2 to 59.7 W/m^2 , the Cu(II)
 4 photoreduction rate increases.

5 **A parallel increase of BA oxidation rate was also observed (data not shown). The results**
 6 **collected during these runs indicate that, under controlled temperature and irradiance, no S-**
 7 **shaped concentration profile was recorded.**

8

9 3.4 Figure-of-merit

10 To estimate the operating costs of sole natural radiation, the figure-of-merit concept was used [33].

11 For solar-energy-driven systems, the figure-of-merit allows the assessment of the solar technology
 12 efficiency used for the investigated process. In fact, even if there is no cost for solar radiation, there
 13 could be a non-marginal capital cost for the collector. Being the capital cost of a solar collector
 14 generally proportional to its area, a figure-of-merit, based on the solar collector area, is appropriate.

15 For the adopted experimental batch conditions, the appropriate figure-of-merit is the collector area
 16 per mass (A_{CM}), defined as the collector area required to reduce of a unit mass of the substrate in the
 17 reacting system in a time of 1 hour (t_o) for an incident solar irradiance of 1000 W m^{-2} (E_S^o):

$$A_{CM} = \frac{1000 \cdot A_r \cdot t \cdot \overline{E_S}}{M \cdot V_t \cdot t_o \cdot E_S^o \cdot (c_i - c_f)} \quad \text{eq. 3}$$

18 where A_r (3.19 m^2) is the real collector area, M is the molar mass of the substrate (108.14 g/mol), V_t
 19 (39 l) is the volume of treated solution, $\overline{E_S}$ (814.6 W/m^2) is the average direct solar irradiance over
 20 the reaction time t (4.83 h), c_i and c_f are respectively the initial and final substrate concentrations

1 (mol/l), E_s^0 is the standardized irradiance (1000 W/m^2 , based on the AM1.5 standard solar spectrum
2 on a horizontal surface) [34] and t_0 is the reference time (1 h).

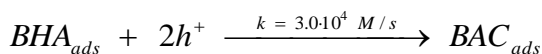
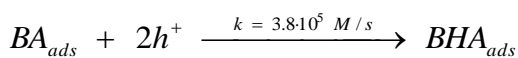
3 On the basis of the previous formula an average value of $A_{CM} = 3.08 \cdot 10^3 \text{ m}^2$ per kilogram of benzyl
4 alcohol and per hour consumed was thus calculated for the collector area per mass (200 mg/l of
5 Aldrich TiO_2 , pH=2.0, $[\text{Cu(II)}]_0 = 1.0 \text{ mM}$, $[\text{BA}]_0 = 1.5 \text{ mM}$).

6

7 3.5 Copper reuse

8 The possibility of reuse the reduced copper, as catalyst, was tested by carrying out an experimental
9 run, by using the CPC solar reactor, consisting in three cycles of BA photo-oxidation (fig. 9). When
10 all Cu(II) species was totally reduced as precipitate copper, its reoxidation was carried out, in dark
11 conditions, under air bubbling in the recirculation tank for 30 minutes. At the end of the first cycle,
12 the reactive solution was re-purged with nitrogen gas, for other 30 minutes, to remove the dissolved
13 oxygen and a new photocatalytic cycle was started. The experimental results, reported in figure 9,
14 pointed out that it's possible, for each cycle, to reoxidize completely the precipitate copper to cupric
15 species (empty diamonds).

16 During the first two cycles of BA solar photooxidation, not particular changes were observed on the
17 reactivity of the system, whereas during the third cycle a decrease of both BA consumption and
18 BHA production rates were observed. This behaviour could be explained by considering that the
19 solution composition changes during the experimental run. In particular, at the 3rd cycle beginning,
20 BA **conversion** and BHA **yield** were 43% and 33% respectively thus favouring a competition
21 kinetics between BA and BHA, both adsorbed on TiO_2 surface, towards the reaction with the
22 photogenerated holes [35]:



1 The BHA selectivities of the process for the three photocatalytic cycles are reported in figure 10. As
2 shown in the diagram, the highest selectivities (up to 100%) were obtained in the first cycle,
3 whereas lower selectivities were observed during the second (close to 75%) and the third cycle
4 (close to 40%), thus supporting, with the progress of the reaction time, the intervention of undesired
5 oxidation reactions of BHA once produced.

6 After each photocatalytic cycle under anoxic conditions, the solid was filtered, stored under inert
7 atmosphere and submitted to EDS, XRD and XPS analysis in order to better investigate the
8 distribution of copper deposited on the solid and its oxidation states.

9 From the EDS investigations, Ti/Cu atom ratios, for the filtered solids, resulted 97.8/2.2, 96.5/3.5
10 and 85.2/14.8 (w/w) for the samples withdrawn at the end of the first, second and third cycle
11 respectively. These results supported the idea that reduced Cu species, formed during the photo-
12 oxidative runs, accumulated on TiO₂ surface increasing the amount of deposited copper from the
13 first cycle to third one up to 17.4% by weight. The increase of Cu amount on the TiO₂ is probably
14 due to the deposition of a part of photocatalyst powders, during the experimental run, in the
15 recirculation tank and/or along the hydraulic connections of the plant, thus decreasing the active
16 load of it available in the solar photoreactor with a consequent reduction of BA consumption and
17 BHA production rates, really observed, in particular during the third cycle.

18 A typical XPS spectra for the solid samples shows different peaks (fig. 11). The peaks at 932.8 eV
19 and 952.6 eV indicate the predominant presence of copper reduced species (+1/0) as previously
20 reported by others [19,22,36] whereas the existence of peaks at 935.4 eV and 955.2 eV can be
21 attributed to the presence of cupric species [22], such as CuO, probably an artifact produced during
22 the preparation of the sample before the XPS analysis.

23 Unfortunately, XRD analysis did not give any result being the amount of Cu reduced species
24 accumulated on the TiO₂ surface (max 17.4%) below XRD detection limit.

25

26

1 **4. Conclusion**

2 The possibility to convert benzyl alcohol to benzaldehyde by photocatalytic oxidation was
3 demonstrated in aqueous solution under natural solar radiation at pilot plant scale. The oxidation
4 rates were strongly influenced by the initial cupric ions concentration, incident solar irradiance and
5 temperatures. The best result found, in terms of yield, was of 53.3% for benzaldehyde with respect
6 to the initial benzyl alcohol concentration (63.4 % of selectivity) for an accumulated energy value
7 (Q_n) of 78.9 kJ/l (reaction time of 385 min) and operating with an average temperature of 38.6 °C.

8 EPS investigations, carried out on the solids, withdrawn during different photocatalytic cycles,
9 confirmed the existence of both Cu reduced (0/+1) and oxidized species, the latter probably
10 produced during the sample preparation before the analysis.

11 The results also indicated that cupric species can be easily regenerated and reused with air or
12 oxygen in dark conditions.

13 A figure-of-merit (A_{CM}) was calculated be equal to $3.08 \cdot 10^3$ m² per kilogram and hour of benzyl
14 alcohol converted.

15

16 **References**

17 [1] M.N. Chong, B. Jin, C.W.K. Chow, C. Saint, *Water Research* 44 (2010) 2997 – 3027.

18 [2] K. Rajeshwara, M.E. Osugi, W. Chanmanee, C.R. Chenthamarakshan, M.V.B Zaroni, P.
19 Kajitvichyanukul, R. Krishnan-Ayer, *Journal of Photochemistry and Photobiology C:*
20 *Photochemistry Reviews* 9 (2008) 171–192.

21 [3] J.M. Herrmann, *Applied Catalysis B-Environmental* 99(3-4) (2010) 461-468.

22 [4] R.J. Braham, A.T. Harris, *Industrial & Engineering Chemistry Research*, 48 (2009) 8890–8905.

23 [5] S.R. Malato, P. Fernandez-Ibanez, M.I. Maldonado, G.J. Blanco, W. Gernjak, *Catalysis Today*
24 147 (2009) 1–59.

25 [6] Y. Shiraishi, T. Hirai, *Journal of Photochemistry and Photobiology C: Photochemistry Reviews*
26 9 (2008) 157–170.

- 1 [7] S. Higashimoto, N. Suetsugu, M. Azuma, H. Ohue, Y. Sakata, *Journal of Catalysis* 274 (2010)
2 76–83.
- 3 [8] W. Feng, G. Wu, L. Li, N. Guan, *Green Chemistry* 13 (2011) 3265–3272.
- 4 [9] C.S. Turchi, D.F. Ollis, *Journal of Catalysis*, 122 (1990) 178–192.
- 5 [10] S. Higashimoto, N. Kitano, N. Yoshida, T. Sakura, M. Azuma, H. Ohue, Y. Sakata, *Journal of*
6 *Catalysis* 266 (2009) 279–285.
- 7 [11] G. Palmisano, S. Yurdakal, V. Augugliaro, V. Loddo, L. Palmisano, *Adv. Synth. Catal.* 349
8 (2007) 964-970.
- 9 [12] S. Yurdakal, G. Palmisano, V. Loddo, V. Augugliaro, L. Palmisano, *Journal of American*
10 *Chemical Society* 130 (2008) 1568-1569.
- 11 [13] V. Augugliaro, V. Loddo, M.J. Lopez-Munoz, C. Marquez-Alvarez, G. Palmisano, L.
12 Palmisano, S. Yurdakal, *Photochemical & Photobiological Sciences* 8 (2009) 663–669.
- 13 [14] R. Marotta, I. Di Somma, D. Spasiano, R. Andreozzi, V. Caprio, *Chemical Engineering*
14 *Journal* 172 (2011) 243–249.
- 15 [15] J.W.M. Jacobs, F.W.H. Kampers, J.M.G Rikken, C.W.T. Bulle-Lieuwma, D.C. Doningsberger,
16 *Journal of The Electrochemical Society* 136 (1989) 2914-2023.
- 17 [16] M. Bideau, B. Claudel, L. Faure, M. Rachimoallah, *Chemical Engineering Communications* 93
18 (1990) 167–179.
- 19 [17] S. Morishita, *Chemistry Letters* 10 (1992) 1979-1982.
- 20 [18] N.S. Foster, R.D. Noble, C.A. Koval, *Environmental Science & Technology* 27 (1993) 350–
21 356.
- 22 [19] S.W. Zou, C.W. How, J.P. Chen, *Industrial & Engineering Chemistry Research* 46(20) (2007)
23 6566–6571.
- 24 [20] M. Canterino, I. Di Somma, R. Marotta, R. Andreozzi, . *Water Res.*, 42 (2008) 4498 -4506.
- 25 [21] H. Reiche, W.W. Dunn, A.J. Bard, *Journal of Physical Chemistry* 83 (1979) 2248-2251.

- 1 [22] S. Xu, J. Ng, A.J. Du, J. Liu, D.D. Sun, *International Journal of Hydrogen Energy* 36 (2011)
2 6538-6545.
- 3 [23] D.I. Enache, J.K. Edwards, P. Landon, B. Solsona-Espriu, A.F. Carley, A.A. Herzing, M.
4 Watanabe, C.J. Kiely, D.W. Knight, G.J. Hutchings, *Science* 311 (2006) 362–365.
- 5 [24] S. Yurdakal, G. Palmisano, V. Loddo, O. Alagoz, V. Augugliaro, L. Palmisano, *Green Chem.*
6 11 (2009) 510–516.
- 7 [25] V. Augugliaro, T. Caronna, V. Loddo, G. Marci, G. Palmisano, L. Palmisano, S. Yurdakal,
8 *Chemistry - A European Journal*. 14 (2008) 4640–4646.
- 9 [26] S. Higashimoto, K. Okada, T. Morisugi, M. Azuma, H. Ohue, T.H. Kim, M. Matsuoka, M.
10 Anpo, *Topics in Catalysis* 53 (2010) 578–583.
- 11 [27] C.J. Li, G.R. Xu, B. Zhang, J.R. Gong, *Applied Catalysis B: Environmental* 115–116 (2012)
12 201–208.
- 13 [28] L. Prieto-Rodriguez, S. Miralles-Cuevas, I. Oller, A. Agüera, G. Li Puma, S. Malato, *Journal*
14 *of Hazardous Materials* 211– 212 (2012) 131– 137.
- 15 [29] M. Kositzki, I. Poulios, S. Malato, J. Cáceres, A. Campos, *Water Research*, 38 (2004) 1147-
16 1154.
- 17 [30] S. Malato, J. Blanco, C. Richter, M.I. Maldonado, *Applied Catalysis B: Environmental* 25
18 (2000) 31–38.
- 19 [31] M. Abdullah, G.K.C. Low, R.W. Matthews, *Journal of Physical Chemistry* 94 (1990) 6820–
20 6825.
- 21 [32] J. Colina-Márquez, F. Machuca-Martínez, G. Li Puma, *Environmental Science & Technology*
22 44 (2010) 5112–5120.
- 23 [33] J.R. Bolton, K.G. Bircher, W. Tumas, C.A. Tolman, *Pure and Applied Chemistry*, 73(4)
24 (2001) 627–637.
- 25 [34] R. Hulstrom, R. Bird, C. Riordan, *Solar Cells* 15 (1985) 365–391.

- 1 [35] R. Marotta, D. Spasiano, I. Di Somma, R. Andreozzi, V. Caprio, *Chemical Engineering*
- 2 *Journal*, 209 (2012) 69-78.
- 3 [36] C.C. Chusuei, M.A. Brookshier, D.W. Goodman, *Langmuir* 15 (1999) 2806-2808.
- 4 **[37] D. Chen, A.K. Ray, *Chemical Engineering Science* 56 (2001) 1561–1570.**

1 **TiO₂/Cu(II) photocatalytic production of benzaldehyde from benzyl**
2 **alcohol in solar pilot plant reactor**

3 Danilo Spasiano^{a*}, Lucia del Pilar Prieto Rodriguez^b, Jaime Carbajo Olleros^c, Sixto Malato^b,
4 Raffaele Marotta^a, Roberto Andreozzi^a

5
6 ^a Department of Chemical Engineering, Faculty of Engineering, University of Naples “Federico II”,
7 p.le V. Tecchio, 80 – 80125 – Naples, Italy.

8 ^b Plataforma Solar de Almería-CIEMAT, Carretera de Senés Km 4 - 04200 - Tabernas, Almería,
9 Spain.

10 ^c Departamento de Ingeniería de Procesos Catalíticos Instituto de Catálisis y Petroleoquímica, CSIC,
11 C/ Marie Curie 2 - 28049 - Cantoblanco, Madrid, Spain.

12
13
14 * Corresponding author. Tel +390817682968 fax +390815936936. E-mail danilo.spasiano@unina.it

15

16 **ABSTRACT**

17 The technical feasibility of selective photocatalytic oxidation of benzyl alcohol to benzaldehyde, in
18 aqueous solutions, in presence of cupric ions has been investigated in a solar pilot plant with
19 Compound Parabolic Collectors. Aldrich (pure anatase) and P25 Degussa TiO₂ have been used as
20 photocatalysts. The influences of cupric species concentrations, solar irradiance and temperature are
21 discussed too. The oxidation rates were strongly influenced by the initial cupric ions concentration,
22 incident solar irradiance and temperatures.

23 The best results found, in terms of yields and selectivities to benzaldehyde under acidic conditions
24 were higher than 50% and 60% respectively under acidic conditions.

1 Under deaerated conditions, the presence of reduced copper species was proved by XPS analysis.
2 The results indicated that, at the end of the process, cupric species can be easily regenerated and
3 reused, through a re-oxidation of reduced copper, produced during the photolytic run, with air or
4 oxygen in dark conditions.

5 A figure-of-merit (A_{CM}), proposed by the International Union of Pure and Applied Chemistry
6 (IUPAC) and based on the collector area, has been estimated, under the proposed conditions, with
7 the aim to provide a direct link to the solar-energy efficiency independently of the nature of the
8 system. Generally speaking, it can be considered that lower A_{CM} values higher the system
9 efficiency.

10

11 *Keywords:* selective oxidation, benzyl alcohol, benzaldehyde production, TiO₂ photocatalysis, solar
12 photocatalytic plant, figure-of-merit.

13

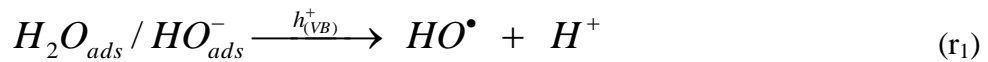
14 **1. Introduction**

15 The use of TiO₂, as readily available and environmentally friendly photocatalyst, was largely
16 investigated for the removal of non-biodegradable or undesirable organic substances from
17 wastewater [1-3] and TiO₂ based on solar technologies were developed during the past years for
18 reducing the cost of large-scale aqueous-phase applications to treat industrial wastewater [4,5].
19 However, only in recent years the research has pointed its attention on the possibility to use the
20 TiO₂ as a photocatalyst for the selective oxidation of organic molecules under UV radiation in non
21 aqueous media [6]. For example, the selective oxidation of aromatic alcohols in the respective
22 aldehydes can be easily gained in acetonitrile or in solvent free systems at room temperature [7,8]
23 due to the reaction of the alcoholic substrate with the photogenerated positive holes (h_{vb}^+) and using
24 oxygen as acceptor of photoelectrons [9]. In particular, the addition of an organic solvent, as
25 acetonitrile, allows the oxidation of benzyl alcohol and its derivatives with selectivities to the

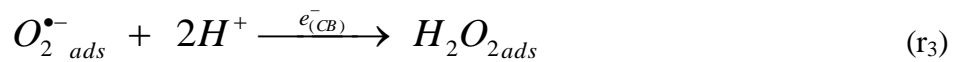
1 respective aldehydes of over 90% [8,10], values well higher than those reported (10-60%) when the
2 same process is carried out in aqueous solutions using TiO₂ nanoparticles [11,12].

3 Moreover, selectivities of 41-74% were reported for the oxidation of 4-substituted aromatic
4 alcohols to the corresponding aldehydes, using aqueous media, over rutile or anatase TiO₂ catalysts
5 [11,13]. The decrease of the selectivity in aqueous solution with respect the use of organic non
6 aqueous solvent is mainly due to [9]:

7 a) formation of very reactive species such as hydroxyl radicals (HO[•]) through the reaction of
8 adsorbed water molecules or hydroxyl groups with positive holes:

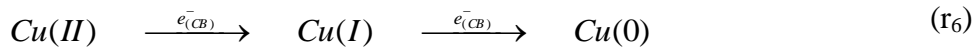


9 b) generation of radical superoxide (O₂^{•-}) by the reaction of molecular oxygen with photogenerated
10 electrons (e_{cb}⁻). This species, once formed, in presence of water, gives rise hydrogen peroxide
11 whose electron trapping generates HO[•] radicals, which, in absence of non aqueous solvent, oxidizes
12 not selectively the organic substances:



13 On the other side, water is considered the best solvent for environmental friendly process and, for
14 this reason, other new approaches have arisen in order to avoid the use the organic solvents. In
15 particular, very recent studies demonstrated that the use of Cu(II) ions, as electron acceptor, instead
16 of molecular oxygen, under deaerated conditions, leads to an increase of selectivity to benzaldehyde
17 up to 72%, starting from benzyl alcohol [14], since the formation of hydroxyl radicals takes place
18 just by the reaction of water molecules or surface adsorbed hydroxyl groups with positive holes. In

1 this case, cupric ions reduce to a lower state of oxidation by capturing the photogenerated electron
2 on the TiO₂ surface and precipitate from the solution:



3 whereas adsorbed benzyl alcohol (BA) is oxidized to the benzaldehyde (BHA), through a direct
4 reaction with the positive holes:



5 At the end of the process, cupric ions could be regenerated and reused, through the reoxidation of
6 zero valent precipitated copper with an air flow at dark conditions.

7 Chemical state of solid copper after the photocatalytic run was also intensively investigated, but
8 controversial results were reported. Most of the researchers reported that the solid is composed by a
9 mixture of zero valent copper and cupric oxide (and, in some case, cuprous oxide) [15-19].

10 In some studies it was concluded that the reduced Cu species was zero valent copper [20-21].
11 However, the possibility of the presence of both Cu(I)/Cu(II) species, due to a reoxidation of metal
12 copper during the preparation of the analytical samples, was not completely ruled out [22].

13 At best of the Authors' knowledge, only lab-scale lamp-driven investigations on the selective TiO₂
14 photocatalytic oxidation of benzyl alcohol and its derivatives, in aqueous or acetonitrile or solvent
15 free systems, were reported in the literature [11, 12, 14, 23-27].

16 It could be very interesting, for economic and environmental reasons, to evaluate the possibility of
17 exploiting the use of solar radiations dayling arriving on the earth surface, through the use of pilot
18 plants, for the production of benzaldehyde from benzyl alcohol.

19 In the present work, the development of the TiO₂/Cu(II)/solar radiation system for the selective
20 oxidation of benzyl alcohol to benzaldehyde in water is studied, by using a solar photocatalytic pilot
21 plant at different operating conditions (TiO₂ photocatalyst type, Cu(II) initial concentration and
22 irradiance of solar radiation). The possibility of reuse copper as catalyst was also tested by
23 oxidizing the precipitated zero valent copper with an air flow blown into the pilot-plant in dark

1 conditions. Optimal conditions of TiO₂ load and pH values were fixed according to the ones found
2 in previous studies [14,28].

3 Moreover, analyses of solid, after the oxidation runs, were carried out to better clarify the nature of
4 copper species at the end of the process.

5

6 **2. Material and methods**

7 *2.1 Experimental set-up and procedures*

8 *2.1.1 Pilot-Plant experiments*

9 Experimental investigations were carried out, from May to July 2012, in a solar pilot-plant
10 consisting of twelve Compound Parabolic Collectors (CPC), installed in the Plataforma Solar de
11 Almería (37° latitude N, Spain) and elsewhere described in its geometrical and functional
12 characteristics [29]. The total solution volume is 39 l, where only 22 l are exposed to solar
13 radiation; the rest is distributed between the recirculation tank (9 l) and the hydraulic connections (8
14 l). The recirculation tank of the adopted CPC was modified, as reported in figure 1, in order to
15 ensure the absence of oxygen, essential for performing the proposed process. For this purpose, the
16 solutions, containing the catalysts and the substrate, were preventively purged with nitrogen
17 gaseous stream through two porous ceramic spargers, by closing the valve V_n, to remove the
18 dissolved oxygen. During the experimental runs a continuous nitrogen flow was guaranteed to the
19 reactor to prevent the entry of air in the reactor but it was switched in the freeboard of the
20 recirculation tank, by opening the valve V_n, to inhibit the stripping of organic substances from the
21 solution. In the last case, the bubbling of nitrogen is strongly limited by the pressure drop due to the
22 spargers.

23 To better follow the concentration profiles of the compounds involved in the process, some
24 experimental runs were carried out during two days. In these cases, the irradiated part of the reactor
25 was covered and the recycling tank was capped to stop the photochemical reactions and to prevent
26 the entry of oxygen respectively.

1 Samples were collected in a glass bottle at different reaction times, by opening the valve V_s , rapidly
2 filtered to prevent the reoxidation of precipitate copper and finally analyzed.

3 All the experimental data were reported in function of the accumulated energy, per unit of volume
4 (kJ/l), incident on the reactor at the corresponding time of the withdrawn sample (Q_n) [30]:

$$Q_n = Q_{n-1} + \Delta t_n \cdot \overline{UV}_n \cdot \frac{A_r}{V_t}; \quad \Delta t_n = t_n - t_{n-1} \quad (\text{eq. 1})$$

5 where Q_{n-1} represent the accumulated energy (per unit of volume, kJ/l) taken during the experiment
6 relative to the previous sampling; Δt_n , \overline{UV}_n and V_t are, respectively, the elapsed time, the average
7 UV-irradiance (measured by a global UV radiometer KIPP&ZONEN, model CUV 3 mounted on a
8 platform tilted the same angle as the CPCs) which reaches the collector surface (A_r) between the
9 two samplings and the total solution volume.

10

11 *2.1.2 Laboratory-scale experiments*

12 Experiments were carried out in a Suntest solar simulator (Suntest XLS+ photoreactor, Atlas)
13 equipped with a 765-250 W/m² Xenon lamp (61-24 W/m² from 300 nm to 400 nm, $1.4 \cdot 10^{20}$ -
14 $5.5 \cdot 10^{19}$ photons/m²·s) and a cooler to keep the temperature at 35°C. The UV irradiation, in the
15 range of 300-400 nm, was monitored by using a portable radiometer (Solar Light CO PMA 2100)
16 fixed on the shaker inside the lamp influence zone, like shown in figure 2.

17 In this case, a volume of 700 ml of reacting solution was prepared in a one liter flask and, after 30
18 minutes of stripping with nitrogen, was rapidly poured in ten cylindrical glass vials with the
19 capacity of 42 ml and a diameter of 25 mm. The vials were rapidly closed with a screw cap, to
20 prevent the entry of oxygen, and were simultaneously exposed to the lamp radiation and agitated by
21 a shaker like shown in figure 2. The temperature was set at 35 °C. Each vial represented a sample to
22 remove from the solar box at different reaction times. Once collected, all the samples were rapidly
23 filtered and analyzed.

1 The pH of the solutions was adjusted at the value of 2.0, for all the runs, by using an aqueous
2 solution of 85% of phosphoric acid.

3 *2.2 Analytical methods*

4 The concentrations of benzyl alcohol, benzaldehyde and benzoic acid at different reaction times
5 were evaluated by HPLC analysis. For this purpose, the HPLC apparatus (Agilent 1100) was
6 equipped with a diode array UV/Vis detector ($\lambda = 215, 230, 250$ nm) and Phenomenex (Gemini 5u
7 C18 150x3 mm) column, using a mobile phase flowing at 0.7 ml min^{-1} . The mobile phase was
8 prepared by a buffer solution (A), H₂O (B) and CH₃CN (C). A linear gradient progressed from 15%
9 C to 28% C and from 45% B to 32% B in 10 minutes with a subsequent re-equilibrium time of 3
10 minutes. One liter of buffer was made by 10 ml of phosphoric acid solution (5.05 M), 50 ml of
11 methyl alcohol and water for HPLC.

12 The concentration of dissolved copper ions was measured by means of a colorimetric method using
13 an analytical kit (based on oxalic acid bis-cyclohexylidene hydrazide, cuprizone®) purchased from
14 Macherey-Nagel. An UV/Vis spectrometer (UNICAM-II spectrophotometer) has been used for the
15 measurements at a wavelength of 585 nm.

16 Total organic carbon (TOC) was monitored by Shimadzu Total Organic Carbon analyser model
17 TOC-5050A, equipped with an auto sampler ASI 5000A. The pH was monitored by a portable pH-
18 meter (Crison pH 25).

19 The Cu/Ti ratio for unknown solids, withdrawn at the end of some photocatalytic runs, was
20 estimated by an Energy Dispersive X-ray spectrometer system (SwiftED, Oxford Instruments)
21 attached to a Scanning Electron Microscope (TM-1000, Hitachi).

22 Powder X-ray diffraction (XRD) patterns were estimated using a X'PertPRO (PANalytical)
23 diffractometer with nickel-filtered Cu K α radiation. The X-ray generator was operated at 45 kV and
24 40 mA. The powders were scanned from $2\theta = 4^\circ$ to 90° with a 0.02 step size and accumulating a
25 total of 5 s per point.

1 X-ray photoelectron spectroscopy (XPS) analysis was carried out under high vacuum chamber with
2 a base pressure below 9×10^{-7} Pa at room temperature. Photoemission spectra were recorded using a
3 SPECS Gmbh system equipped with an UHV PHOIBOS 150 analyser with Al monochromatic
4 anode operated at 12 kV and 200 W with a photon energy of $h\nu = 1486.74$ eV. A pass energy of 25
5 eV was used for high-resolution scans. Binding energies (BE) were referenced to C1s peak (284.6
6 eV) to take into account charging effects.

7 The XPS spectra obtained were then curved fitted using the XPS PeakFit software. The areas of the
8 peaks were computed by fitting the experimental spectra to Gaussian/Lorentzian curves after
9 subtracting the background (Shirley function).

10

11 *2.3 Materials*

12 Two commercial microcrystalline TiO₂ powders were tested: TiO₂ Degussa P25 (80% anatase, 20%
13 rutile, BET specific surface area $50 \text{ m}^2 \text{ g}^{-1}$) and TiO₂ Aldrich (pure anatase phase, BET specific
14 surface area $9.5 \text{ m}^2 \text{ g}^{-1}$).

15 Cupric ions were introduced in the system as anhydrous cupric sulphate (Sigma-Aldrich) with a
16 purity >99.0% (w/w). Benzyl alcohol (BA), benzaldehyde (BHA) and benzoic acid (BAC), with a
17 purity >99.0% (w/w), were purchased from Sigma Aldrich and used as received. Phosphoric acid
18 with a purity 85% from Merck as used as received

19

20 **3. Result and discussion**

21 *3.1 Effect of TiO₂ type*

22 The results obtained during different experimental runs of solar photooxidation of benzyl alcohol,
23 with two different typologies of commercial TiO₂ samples, at the same load (200 mg/l), are shown
24 in figures 3a-b.

1 The runs were carried out in two days. At the end of first day, when the reactor was covered, the
2 UV-irradiances (wavelength 300-400 nm) and temperatures decreased (see figs 3a,b). During the
3 runs, measured UV-irradiances ranged between 40 and 50 W/m² approximately (fig. 3b).
4 As shown in the diagrams, the reactivity of the system is higher when TiO₂ P25 by Degussa is used
5 than the TiO₂ Aldrich catalyst. In particular, in presence of P25 Degussa sample (empty symbols),
6 for a Q_n value of 123 kJ/l, the BA concentration approached to zero (figure 3a) and Cu(II) ions were
7 totally reduced (figure 3b), whereas, if Aldrich TiO₂ sample is used (full symbols), about 27% of
8 initial benzyl alcohol and Cu(II) ions were still present in the solution.

9 The higher reactivity observed for the system in presence of P25 Degussa TiO₂ is in disagreement
10 with the results, previously reported [14], that show a similar reactivity when P25 Degussa and
11 Aldrich TiO₂ catalysts were used in presence of an UV radiation emitted by a laboratory
12 thermostated lamp. This discrepancy may be probably due to the different climatic conditions that
13 influenced the temperature trends of the reacting solution, as reported in figure 3a (dotted and dash-
14 dot lines). Moreover, the different reactivities, recorded in the solar experiments, could be also
15 attributed to the differences between the averages of the measured temperatures: 38.6 °C and 34.3
16 °C for runs carried out in presence of Degussa P25 and Aldrich TiO₂ catalysts respectively.

17 Moreover, since P-25 and Aldrich have not the same light absorption characteristics in the range of
18 300-800 nm, another reason could be the different emission spectra between lamp and the sun.

19 The BA solar photocatalytic oxidation resulted in the production of BHA for both the catalysts, as
20 shown in figure 4 (empty and full diamonds) and BAC an undesired product that derives from the
21 reaction between the positive photogenerated holes on the TiO₂ surface and benzaldehyde. BAC
22 yields are also reported the same figure (empty and full triangles).

23 According to the previous results, the highest BHA production rates were gained in presence of P25
24 Degussa TiO₂. Moreover, for accumulated energy values higher than 80 kJ/l, a decrease in BHA
25 yield with respect of initial BA amount, from the value of 53.3% to 45.5%, was observed using P25
26 Degussa TiO₂ samples. This result can be explained by considering a competition in the reaction

1 between the BA and BHA molecules with the photogenerated positive holes on the TiO₂. This is in
2 agreement with the results reported in figure 3a (empty squares), when the accumulated energy
3 reached the value of 83 kJ/l, the unconverted BA concentration was only 16% of its initial
4 concentration. At the same time, a decrease of production rate of BAC (empty triangles, fig. 4) was
5 recorded, being the unreacted Cu(II) concentration only the 22% of the initial one (empty squares,
6 fig 3b).

7 The BHA selectivity, with respect to BA consumption, was calculated for both TiO₂ types (Fig. 5).
8 As shown in the diagram, it seems that the use of Aldrich TiO₂ sample renders the system more
9 selective, reaching, for Q_n values of 130 kJ/l, BHA selectivity values close to 70% and 50% in
10 presence of Aldrich TiO₂ and P25 Degussa respectively. TOC measurements collected during the
11 runs are also reported in figure 5, in terms of mineralization degrees. The trends are very similar,
12 with a degree of mineralization at the end of the experimental runs of 9% and 7% in presence of
13 P25 Degussa and Aldrich TiO₂ respectively.

14

15 *3.2 Effect of cupric ions concentration*

16 To evaluate the effect of Cu(II) initial concentration, some experimental runs of solar photooxidation
17 of benzyl alcohol were carried out with Aldrich TiO₂ at the load of 200 mg/l and pH = 2.0, varying
18 the cupric ions starting concentration (0.5 mM, 1.0 mM and 1.5 mM).

19 As shown in figures 6a-b, the temperatures and UV-irradiance profiles (solid, dashed and dotted
20 lines) are so similar as to be considered equals for the three runs.

21 With Cu(II) and BA starting concentrations of 0.5 mM and 1.5 mM, the BA oxidation stopped for
22 Q_n values close to 35 kJ/l where a complete reduction of cupric ions was observed (full triangles).

23 At the highest Cu(II) initial concentration than 1.5 mM resulted into a decrease of the system
24 reactivity and BA conversion (Fig. 6a, full circles) and, at the same time, the Cu(II) reduction rates
25 decrease. The observed results, according to those previously reported [14], are probably due to a
26 partial catalyst deactivation by the adsorbed sulphate ions which may block the TiO₂ active sites

1 [31]. In fact, since Cu(II) species were added to the reactive solution as cupric sulphate (CuSO_4),
2 increasing the Cu(II) ions initial concentration results into an increase of sulphate concentration too.
3 Moreover, the sulphate anions, at concentration level higher than 1.0 mM, exerted a negative effect,
4 inhibiting the BA photooxidation rates because they are in competition with BA molecules in the
5 reaction with the positive holes [14].

6 In figure 7 are reported the experimental concentration profiles of BHA and BAC (full and empty
7 symbols) that are in agreement with BA concentration trends shown in figure 6a. In particular the
8 best result found, in term of yield, was of 43% for BHA, starting with $[\text{Cu(II)}]_0 = 1.0$ mM, for a
9 accumulated energy value of 67 kJ/l. For all the runs, the selectivity was always higher than 67%
10 and the mineralization degrees were lower than 4.5% (data not shown).

11

12 *3.3 Effect of the irradiance and temperature*

13 As previously shown in the figures 3b and 6b, the Cu(II) concentrations are characterized by a s-
14 shaped profile and, in particular, when the solar UV radiations and reactor temperatures reached the
15 top, a marked increase of Cu(II) reduction rate was observed. With the aim to better assess the
16 relationship between the variability of both irradiances and temperatures during a solar run and the
17 s-shaped of cupric ions concentration profile, a set of three laboratory photolytic experiments, with
18 Cu(II) initial concentration equal to 0.5 mM, were carried out at three different irradiances, kept
19 constant during a single run and under controlled solution temperature ($T=35$ °C). For this purpose,
20 a solar box apparatus, described in the experimental section, was used. Since the internal diameters
21 of CPC solar reactor tubes and the solar box vials are 31 mm and 24 mm respectively, the TiO_2 load
22 that maximizes the adsorption of UV radiation emitted by solar lamp is higher than the one used for
23 solar experiments carried out in CPC reactor.

24 The optimum TiO_2 concentration (c_{cat}), for which the optical thickness equals that of CPC reactor
25 configuration ($\tau=9.12$) can be easily calculated as suggested by others [28,32]:

$$c_{cat} = \frac{\tau}{(\sigma + k) \times d} = 258 \text{ mg/l} \quad \text{eq. 2}$$

1 where σ is the scattering coefficient ($1.295 \cdot 10^3 \text{ m}^2/\text{kg}$), k is the catalyst specific mass absorption
 2 ($1.75 \cdot 10^2 \text{ m}^2/\text{kg}$) and d the internal tube diameter (24 mm).

3 As shown in figure 8, by increasing the UV irradiance from 39.5 W/m^2 to 59.7 W/m^2 , the Cu(II)
 4 photoreduction rate increases.

5 The increase of Cu(II) reduction rate, by increasing UV irradiance, corresponded to the increase of
 6 BA oxidation rate (data not shown). In particular, when the reacting system accumulated about 60
 7 kJ/l, the BA conversion was of 17% and the BHA yield, was close to 14-16% for all the three runs.
 8 Moreover, under controlled temperature and irradiance, no s-shaped concentration was observed.

9

10 3.4 Figure-of-merit

11 To estimate the operating costs of sole natural radiation, the figure-of-merit concept was used [33].
 12 For solar-energy-driven systems, the figure-of-merit allows to the assessment of the solar
 13 technology efficiency used for the investigated process. In fact, even if there is no cost for the solar
 14 radiation, there could be a non-marginal capital cost for the collector. Being the capital cost of a
 15 solar collector generally proportional to its area, a figure-of-merit, based on the solar collector area,
 16 is appropriate.

17 For the adopted experimental batch conditions, the appropriate figure-of-merit is the collector area
 18 per mass (A_{CM}), defined as the collector area required to reduce of a unit mass of the substrate in the
 19 reacting system in a time of 1 hour (t_0) for an incident solar irradiance of 1000 W m^{-2} (E_S^o):

$$A_{CM} = \frac{1000 \cdot A_r \cdot t \cdot \overline{E_S}}{M \cdot V_t \cdot t_0 \cdot \overline{E_S^o} \cdot (c_i - c_f)} \quad \text{eq. 3}$$

20 where A_r (3.19 m^2) is the real collector area, M is the molar mass of the substrate (108.14 g/mol), V_t
 21 (39 l) is the volume of treated solution, $\overline{E_S}$ (814.6 W/m^2) is the average direct solar irradiance over
 22 the reaction time t (4.83 h), c_i and c_f are respectively the initial and final substrate concentrations

1 (mol/l), E_s^0 is the standardized irradiance (1000 W/m^2 , based on the AM1.5 standard solar spectrum
2 on a horizontal surface) [34] and t_0 is the reference time (1 h).

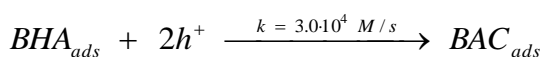
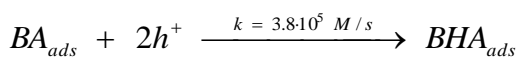
3 On the basis of the previous formula an average value of $A_{CM} = 3.08 \cdot 10^3 \text{ m}^2$ per kilogram of benzyl
4 alcohol and per hour consumed was thus calculated for the collector area per mass (200 mg/l of
5 Aldrich TiO_2 , $\text{pH}=2.0$, $[\text{Cu(II)}]_0 = 1.0 \text{ mM}$, $[\text{BA}]_0 = 1.5 \text{ mM}$).

6

7 *3.5 Copper reuse*

8 The possibility of reuse the reduced copper, as catalyst, was tested by carrying out an experimental
9 run, by using the CPC solar reactor, consisting in three cycles of BA photo-oxidation (fig. 9). When
10 all Cu(II) species was totally reduced as precipitate copper, its reoxidation was carried out, in dark
11 conditions, under air bubbling in the recirculation tank for 30 minutes. At the end of the first cycle,
12 the reactive solution was re-purged with nitrogen gas, for other 30 minutes, to remove the dissolved
13 oxygen and a new photocatalytic cycle was started. The experimental results, reported in figure 9,
14 pointed out that it's possible, for each cycle, to reoxidize completely the precipitate copper to cupric
15 species (empty diamonds).

16 During the first two cycles of BA solar photooxidation, not particular changes were observed on the
17 reactivity of the system, whereas during the third cycle a decrease of both BA consumption and
18 BHA production rates were observed. This behaviour could be explained by considering that the
19 solution composition changes during the experimental run. In particular, at the 3rd cycle beginning,
20 BA and BHA normalized concentrations were 43% and 33% respectively thus favouring a
21 competition kinetics between BA and BHA, both adsorbed on TiO_2 surface, towards the reaction
22 with the photogenerated holes [35]:



1 The BHA selectivities of the process for the three photocatalytic cycles are reported in figure 10. As
2 shown in the diagram, the highest selectivities (up to 100%) were obtained in the first cycle,
3 whereas lower selectivities were observed during the second (close to 75%) and the third cycle
4 (close to 40%) thus supporting, with the progress of the reaction time, the intervention of undesired
5 oxidation reactions of BHA once produced.

6 After each photocatalytic cycle under anoxic conditions, the solid was filtered, stored under inert
7 atmosphere and submitted to EDS, XRD and XPS analysis in order to better investigate the
8 distribution of copper deposited on the solid and its oxidation states.

9 From the EDS investigations, Ti/Cu atom ratios, for the filtered solids, resulted 97.8/2.2, 96.5/3.5
10 and 85.2/14.8 (w/w) for the samples withdrawn at the end of the first, second and third cycle
11 respectively. These results supported the idea that reduced Cu species, formed during the
12 photooxidative runs, accumulated on TiO₂ surface increasing the amount of deposited copper from
13 the first cycle to third one up to 17.4% by weight. The increase of Cu amount on the TiO₂ is
14 probably due to the deposition of a part of photocatalyst powders, during the experimental run, in
15 the recirculation tank and/or along the hydraulic connections of the plant, thus decreasing the active
16 load of it available in the solar photoreactor with a consequent reduction of BA consumption and
17 BHA production rates, really observed, in particular during the third cycle.

18 A typical XPS spectra for the solid samples shows different peaks (fig. 11). The peaks at 932.8 eV
19 and 952.6 eV indicate the predominant presence of copper reduced species (+1/0) as previously
20 reported by others [19,22,36] whereas the existence of peaks at 935.4 eV and 955.2 eV can be
21 attributed to the presence of cupric species [22], such as CuO, probably an artifact produced during
22 the preparation of the sample before the XPS analysis.

23 Unfortunately, XRD analysis did not give any results being the amount of Cu reduced species
24 accumulated on the TiO₂ surface (max 17.4%) below XRD detection limit.

25

26

1 **4. Conclusion**

2 The possibility to convert benzyl alcohol to benzaldehyde by photocatalytic oxidation was
3 demonstrated in aqueous solution under natural solar radiation at pilot plant scale. The oxidation
4 rates were strongly influenced by the initial cupric ions concentration, incident solar irradiance and
5 temperatures. The best result found, in terms of yield, was of 53.3% for benzaldehyde with respect
6 to the initial benzyl alcohol concentration (63.4 % of selectivity) for an accumulated energy value
7 (Q_n) of 78.9 kJ/l (reaction time of 385 min) and operating with an average temperature of 38.6 °C.

8 EPS investigations, carried out on the solids, withdrawn during different photocatalytic cycles,
9 confirmed the existence of both Cu reduced (0/+1) and oxidized species, the latter probably
10 produced during the sample preparation before the analysis.

11 The results also indicated that cupric species can be easily regenerated and reused with air or
12 oxygen in dark conditions.

13 A figure-of-merit (A_{CM}) was calculated be equal to $3.08 \cdot 10^3$ m² per kilogram and hour of benzyl
14 alcohol converted.

15

16 **References**

- 17 [1] M.N. Chong, B. Jin, C.W.K. Chow, C. Saint, *Water Research* 44 (2010) 2997 – 3027.
- 18 [2] K. Rajeshwara, M.E. Osugi, W. Chanmanee, C.R. Chenthamarakshan, M.V.B Zaroni, P.
19 Kajitvichyanukul, R. Krishnan-Ayer, *Journal of Photochemistry and Photobiology C:*
20 *Photochemistry Reviews* 9 (2008) 171–192.
- 21 [3] J.M. Herrmann, *Applied Catalysis B-Environmental* 99(3-4) (2010) 461-468.
- 22 [4] R.J. Braham, A.T. Harris, *Industrial & Engineering Chemistry Research*, 48 (2009) 8890–8905.
- 23 [5] S.R. Malato, P. Fernandez-Ibanez, M.I. Maldonado, G.J. Blanco, W. Gernjak, *Catalysis Today*
24 147 (2009) 1–59.
- 25 [6] Y. Shiraishi, T. Hirai, *Journal of Photochemistry and Photobiology C: Photochemistry Reviews*
26 9 (2008) 157–170.

- 1 [7] S. Higashimoto, N. Suetsugu, M. Azuma, H. Ohue, Y. Sakata, *Journal of Catalysis* 274 (2010)
2 76–83.
- 3 [8] W. Feng, G. Wu, L. Li, N. Guan, *Green Chemistry* 13 (2011) 3265–3272.
- 4 [9] C.S. Turchi, D.F. Ollis, *Journal of Catalysis*, 122 (1990) 178–192.
- 5 [10] S. Higashimoto, N. Kitano, N. Yoshida, T. Sakura, M. Azuma, H. Ohue, Y. Sakata, *Journal of*
6 *Catalysis* 266 (2009) 279–285.
- 7 [11] G. Palmisano, S. Yurdakal, V. Augugliaro, V. Loddo, L. Palmisano, *Adv. Synth. Catal.* 349
8 (2007) 964-970.
- 9 [12] S. Yurdakal, G. Palmisano, V. Loddo, V. Augugliaro, L. Palmisano, *Journal of American*
10 *Chemical Society* 130 (2008) 1568-1569.
- 11 [13] V. Augugliaro, V. Loddo, M.J. Lopez-Munoz, C. Marquez-Alvarez, G. Palmisano, L.
12 Palmisano, S. Yurdakal, *Photochemical & Photobiological Sciences* 8 (2009) 663–669.
- 13 [14] R. Marotta, I. Di Somma, D. Spasiano, R. Andreozzi, V. Caprio, *Chemical Engineering*
14 *Journal* 172 (2011) 243–249.
- 15 [15] J.W.M. Jacobs, F.W.H. Kampers, J.M.G Rikken, C.W.T. Bulle-Lieuwma, D.C. Doningsberger,
16 *Journal of The Electrochemical Society* 136 (1989) 2914-2023.
- 17 [16] M. Bideau, B. Claudel, L. Faure, M. Rachimoellah, *Chemical Engineering Communications* 93
18 (1990) 167–179.
- 19 [17] S. Morishita, *Chemistry Letters* 10 (1992) 1979-1982.
- 20 [18] N.S. Foster, R.D. Noble, C.A. Koval, *Environmental Science & Technology* 27 (1993) 350–
21 356.
- 22 [19] S.W. Zou, C.W. How, J.P. Chen, *Industrial & Engineering Chemistry Research* 46(20) (2007)
23 6566–6571.
- 24 [20] M. Canterino, I. Di Somma, R. Marotta, R. Andreozzi, . *Water Res.*, 42 (2008) 4498 -4506.
- 25 [21] H. Reiche, W.W. Dunn, A.J. Bard, *Journal of Physical Chemistry* 83 (1979) 2248-2251.

- 1 [22] S. Xu, J. Ng, A.J. Du, J. Liu, D.D. Sun, *International Journal of Hydrogen Energy* 36 (2011)
2 6538-6545.
- 3 [23] D.I. Enache, J.K. Edwards, P. Landon, B. Solsona-Espriu, A.F. Carley, A.A. Herzing, M.
4 Watanabe, C.J. Kiely, D.W. Knight, G.J. Hutchings, *Science* 311 (2006) 362–365.
- 5 [24] S. Yurdakal, G. Palmisano, V. Loddo, O. Alagoz, V. Augugliaro, L. Palmisano, *Green Chem.*
6 11 (2009) 510–516.
- 7 [25] V. Augugliaro, T. Caronna, V. Loddo, G. Marci, G. Palmisano, L. Palmisano, S. Yurdakal,
8 *Chemistry - A European Journal*. 14 (2008) 4640–4646.
- 9 [26] S. Higashimoto, K. Okada, T. Morisugi, M. Azuma, H. Ohue, T.H. Kim, M. Matsuoka, M.
10 Anpo, *Topics in Catalysis* 53 (2010) 578–583.
- 11 [27] C.J. Li, G.R. Xu, B. Zhang, J.R. Gong, *Applied Catalysis B: Environmental* 115–116 (2012)
12 201–208.
- 13 [28] L. Prieto-Rodriguez, S. Miralles-Cuevas, I. Oller, A. Agüera, G. Li Puma, S. Malato, *Journal*
14 *of Hazardous Materials* 211– 212 (2012) 131– 137.
- 15 [29] M. Kositzki, I. Poulios, S. Malato, J. Cáceres, A. Campos, *Water Research*, 38 (2004) 1147-
16 1154.
- 17 [30] S. Malato, J. Blanco, C. Richter, M.I. Maldonado, *Applied Catalysis B: Environmental* 25
18 (2000) 31–38.
- 19 [31] M. Abdullah, G.K.C. Low, R.W. Matthews, *Journal of Physical Chemistry* 94 (1990) 6820–
20 6825.
- 21 [32] J. Colina-Márquez, F. Machuca-Martínez, G. Li Puma, *Environmental Science & Technology*
22 44 (2010) 5112–5120.
- 23 [33] J.R. Bolton, K.G. Bircher, W. Tumas, C.A. Tolman, *Pure and Applied Chemistry*, 73(4)
24 (2001) 627–637.
- 25 [34] R. Hulstrom, R. Bird, C. Riordan, *Solar Cells* 15 (1985) 365–391.

- 1 [35] R. Marotta, D. Spasiano, I. Di Somma, R. Andreozzi, V. Caprio, *Chemical Engineering*
- 2 *Journal*, 209 (2012) 69-78.
- 3 [36] C.C. Chusuei, M.A. Brookshier, D.W. Goodman, *Langmuir* 15 (1999) 2806-2808.

Figure 1

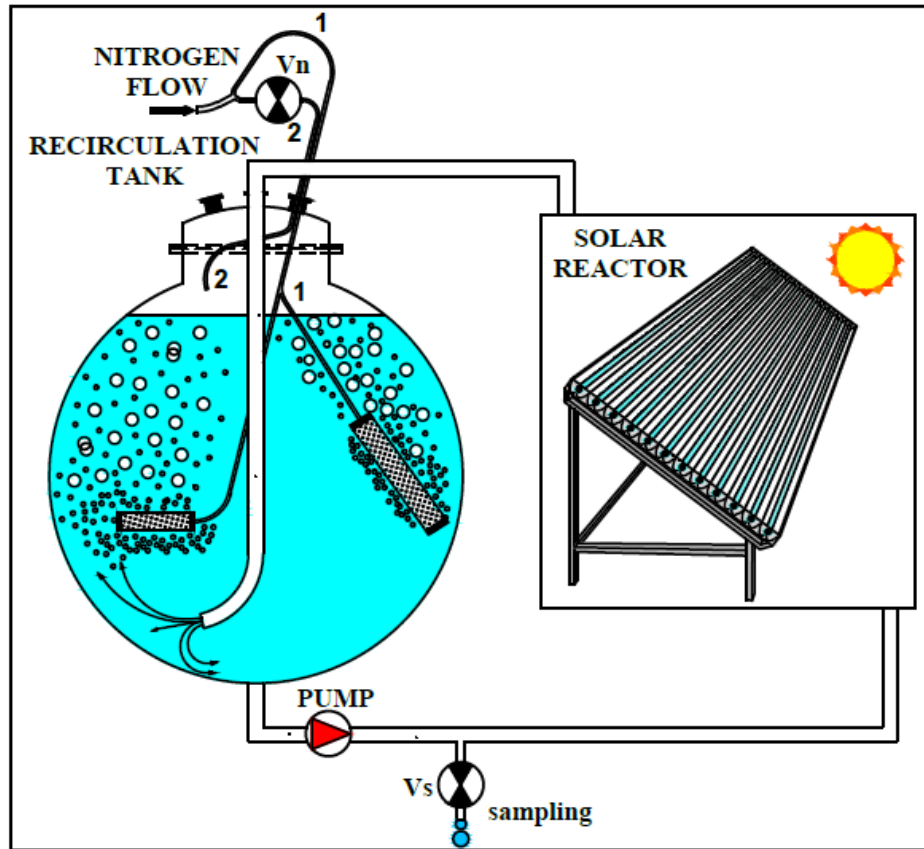


Fig. 1

Figure 2

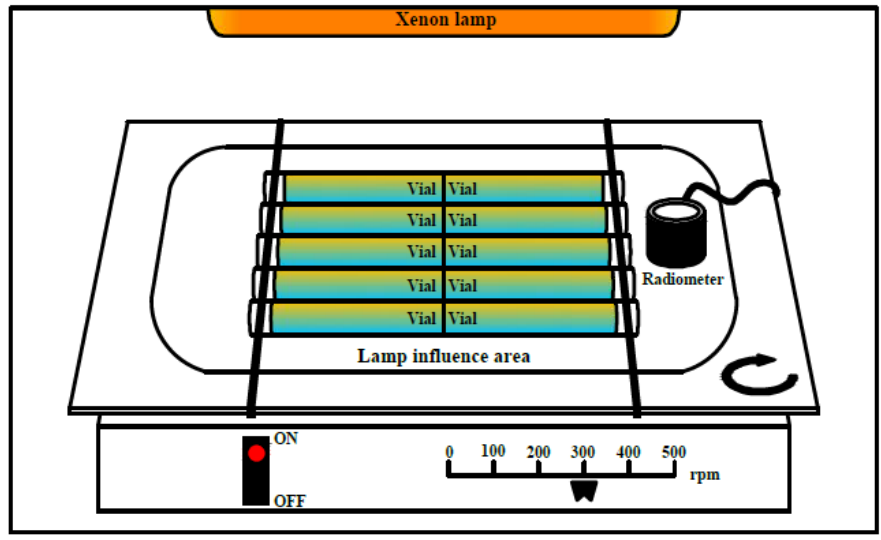


Fig. 2

Figure 3

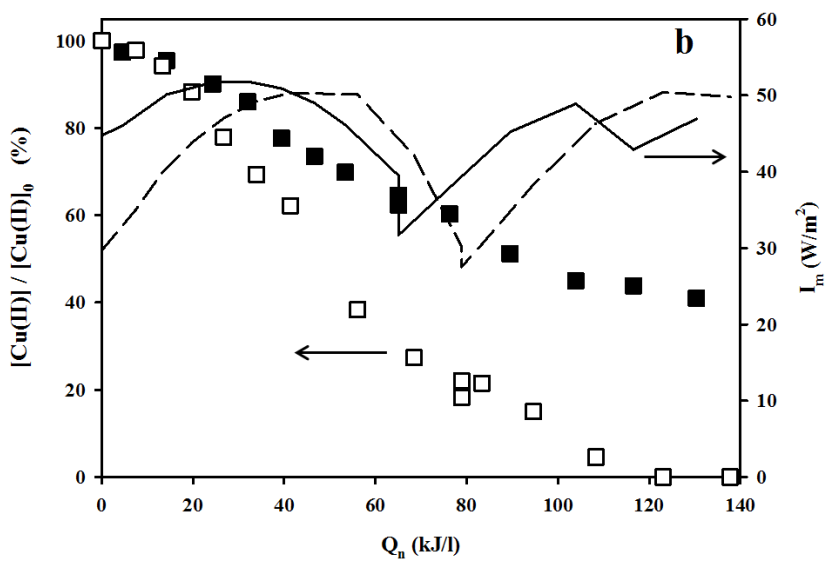
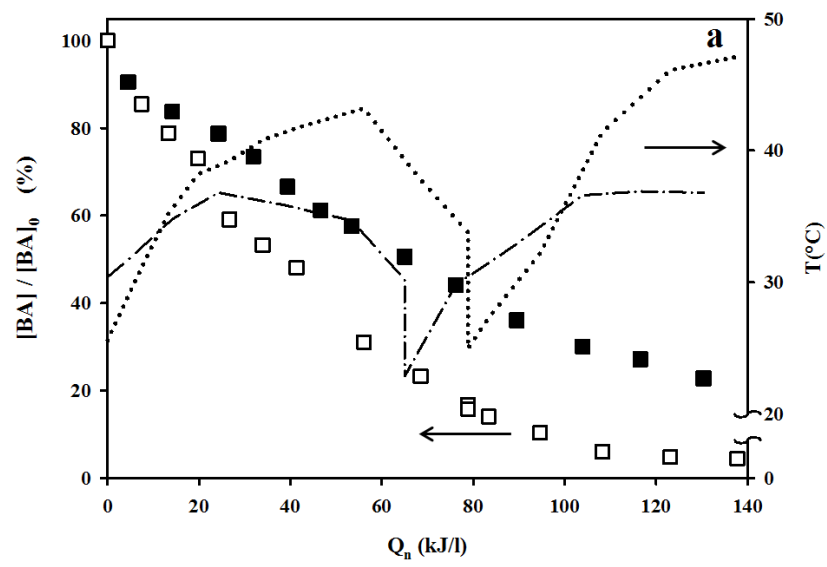


Fig. 3

Figure 4

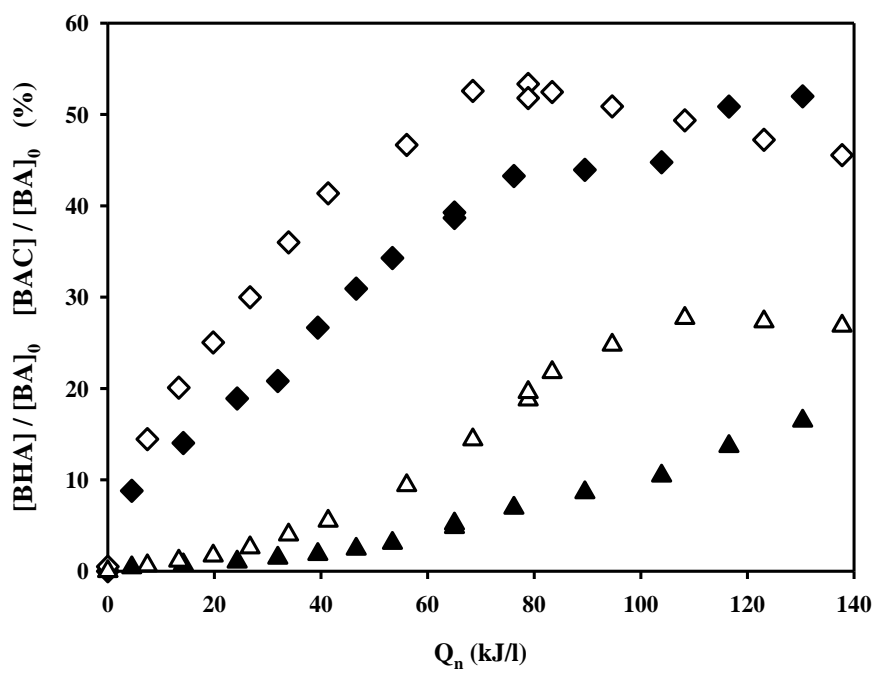


Fig. 4

Figure 5

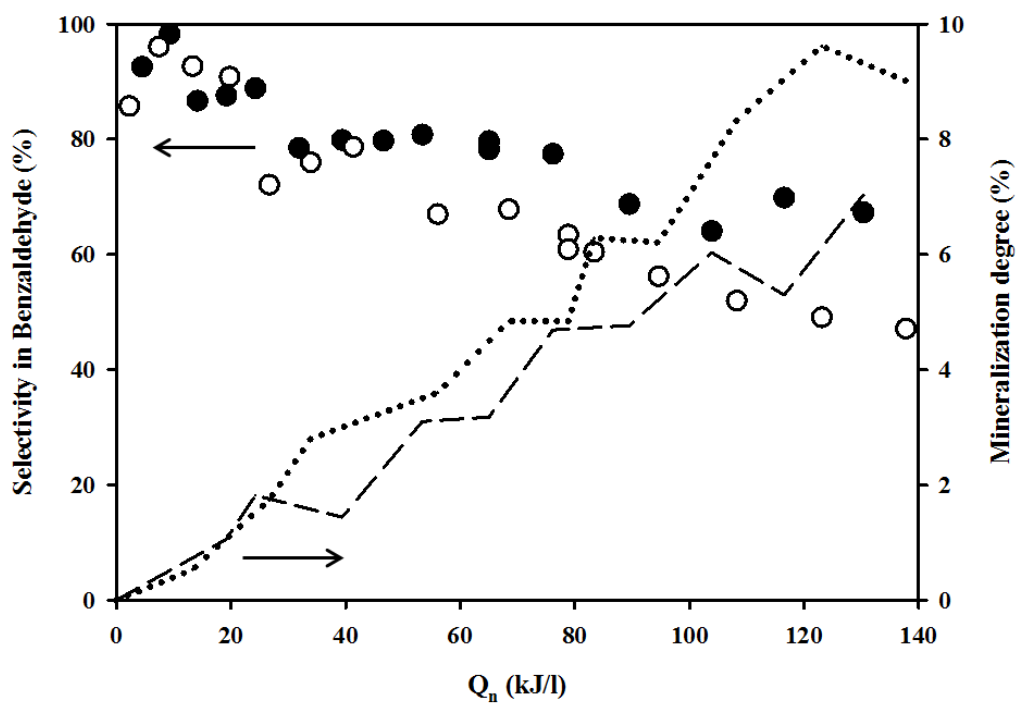


Fig. 5

Figure 6

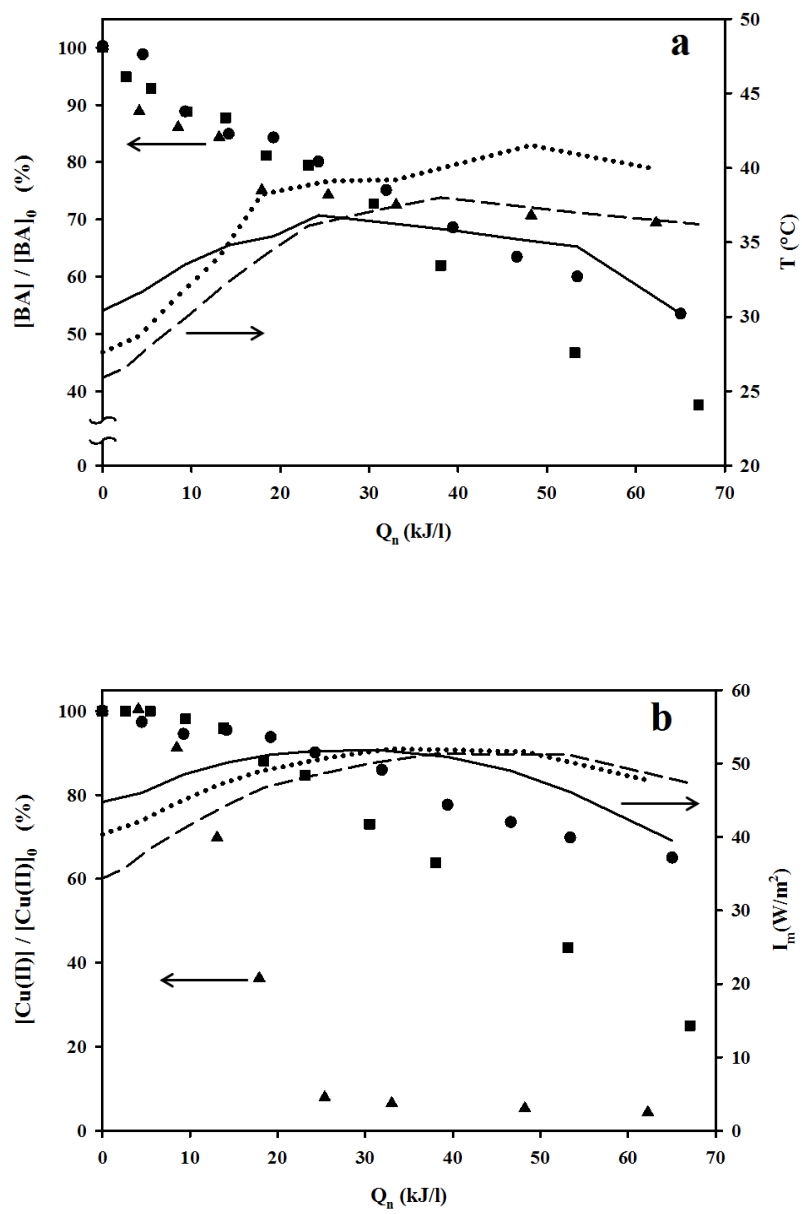


Fig. 6

Figure 7

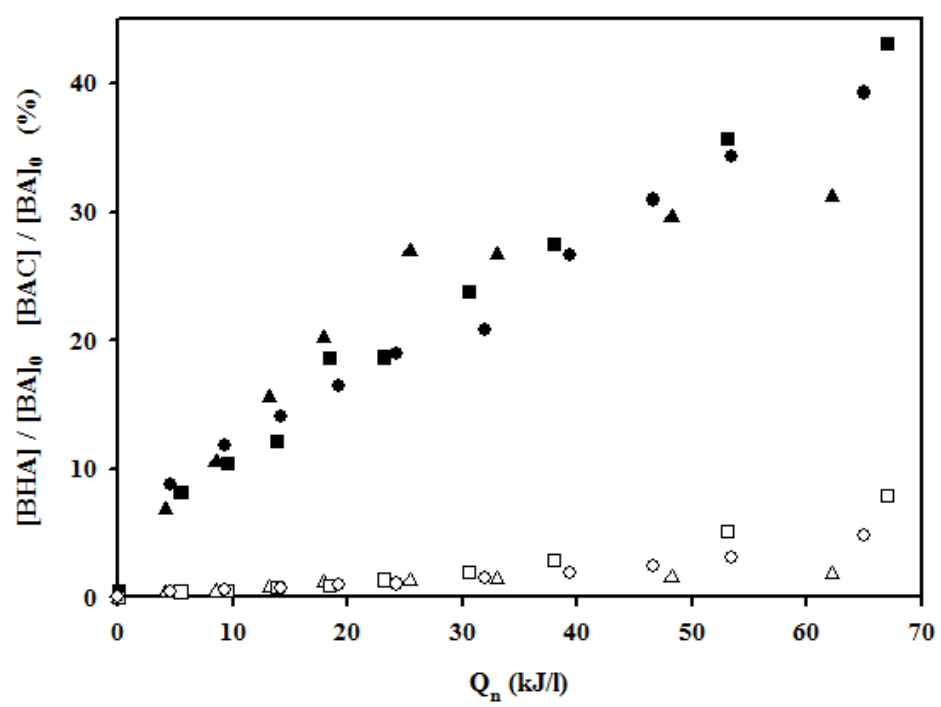


Fig. 7

Figure 8

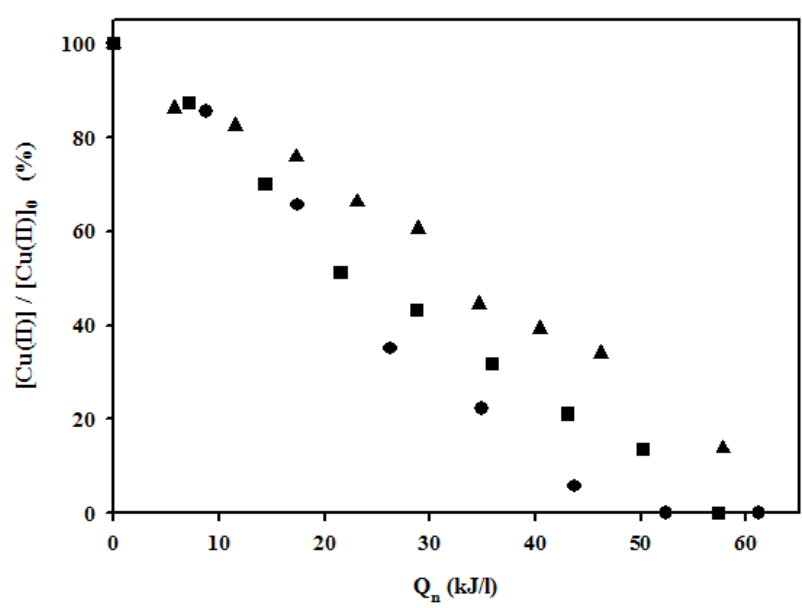


Fig. 8

Figure 9

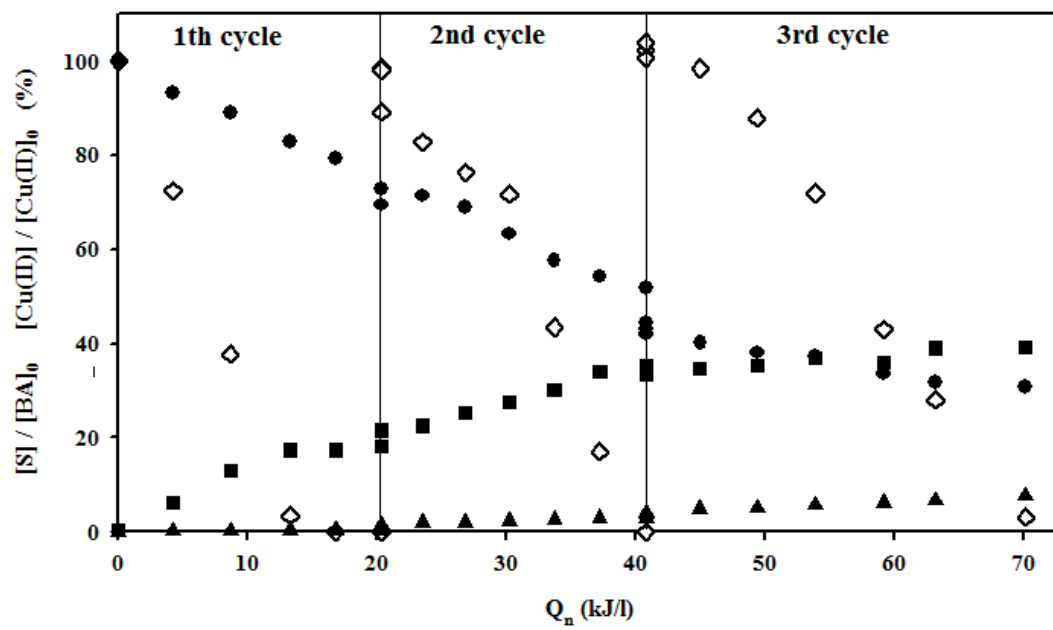


Fig. 9

Figure 10

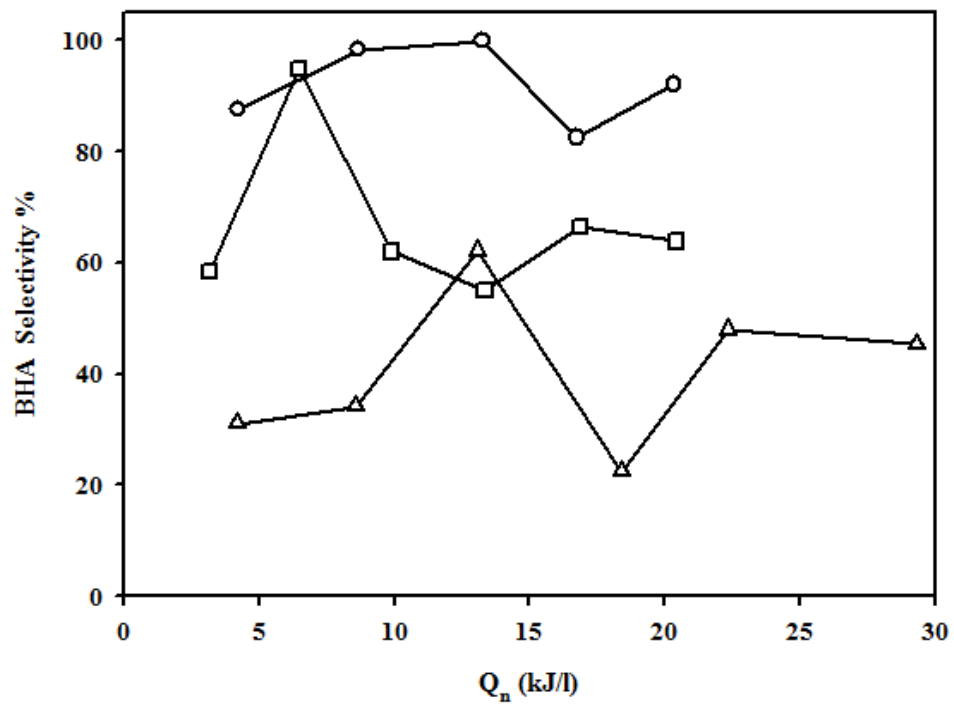


Fig. 10

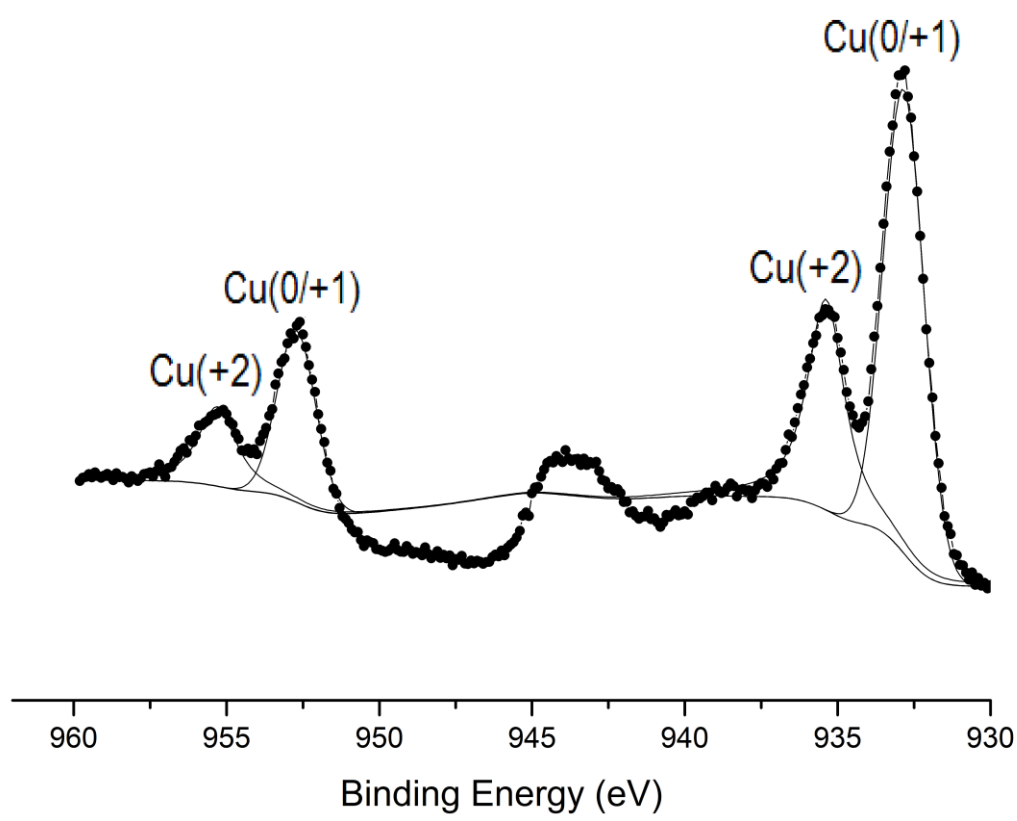


Fig. 11

Fig. 1: Solar photocatalytic CPC pilot plant reactor

Fig. 2: Solar box

Fig. 3: Effect of TiO₂ type at pH=2.0: BA solar photooxidation (squares) and temperatures profiles (dotted and dashed-dotted lines) (**3a**); Cu(II) solar photoreduction (squares) and UV-irradiance (continuous and dashed lines) (**3b**). [BA]₀ = 1.5 mM. [Cu(II)]₀ = 1.5 mM. Initial TiO₂ load = 200 mg/l.

3a: (■, -.-) Aldrich TiO₂, (□, •••) P25 Degussa TiO₂.

3b: (■, —) Aldrich TiO₂, (□, ---) P25 Degussa TiO₂.

Fig. 4: Effect of TiO₂ type on the BHA and BAC production. [BA]₀ = 1.5 mM. [Cu(II)]₀ = 1.5 mM. Initial TiO₂ load = 200 mg/l. pH=2.0.

Aldrich TiO₂: ◆ BHA, ▲ BAC. P25 Degussa TiO₂: ◇ BHA, △ BAC.

Fig. 5: Effect of TiO₂ type on the BHA selectivity and mineralization degree (dotted and dashed lines). [BA]₀ = 1.5 mM. [Cu(II)]₀ = 1.5 mM. Initial TiO₂ load = 200 mg/l. pH=2.0.

Aldrich TiO₂: (●) BHA selectivity, (---) mineralization degree.

P25 Degussa TiO₂: (○) BHA selectivity, (•••) mineralization degree.

Fig. 6: Effect of initial Cu(II) concentration at pH=2.0 on the BA and Cu(II) concentration profiles: BA solar photooxidation and temperatures profiles (**6a**); Cu(II) solar photoreduction and UV-irradiance profiles (**6b**). [BA]₀ = 1.5 mM. Initial TiO₂ (Aldrich) load = 200 mg/l. [Cu(II)]₀: (▲) 0.5 mM, (■) 1.0 mM, (●) 1.5 mM. Temperatures and Irradiances: (•••) for [Cu(II)]₀ = 0.5mM, (---) for [Cu(II)]₀ = 1.0 mM, (—) for [Cu(II)]₀ = 1.5 mM.

Fig. 7: Effect of initial Cu(II) concentration on the BHA and BAC concentration profiles: BHA (full symbols) and BAC (empty symbols) productions. $[BA]_0 = 1.5$ mM. Initial TiO_2 (Aldrich) load = 200 mg/l. pH = 2.0. $[Cu(II)]_0$: ($\blacktriangle, \triangle$) 0.5 mM, (\blacksquare, \square) 1.0 mM, (\bullet, \circ) 1.5 mM.

Fig. 8: Effect of irradiance on the Cu(II) concentration profiles: $[BA]_0 = 1.5$ mM. $[Cu(II)]_0 = 0.5$ mM. Initial TiO_2 (Aldrich) load = 258 mg/l. pH = 2.0 and $T = 35$ °C.

UV Irradiance (solar box): \blacktriangle 39.5 W/m², \blacksquare 49.0 W/m², \bullet 59.7 W/m².

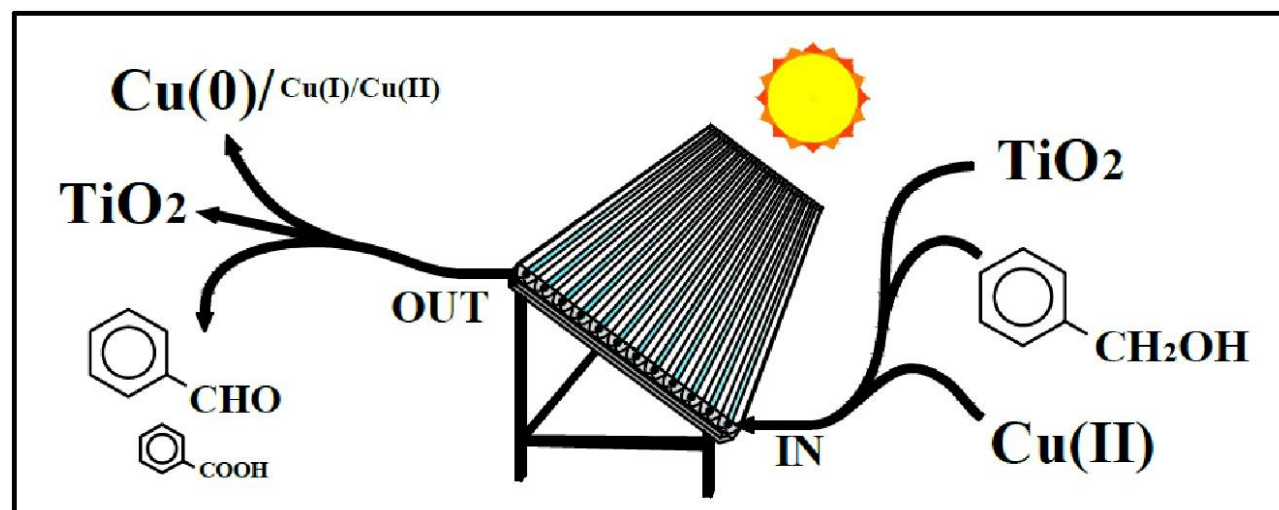
Fig. 9: Normalized concentration profiles for Cu(II), BA, BHA and BAC with light on and nitrogen purge or light off and oxygen purge.

$[BA]_0 = 2.5$ mM. $[Cu(II)]_0 = 0.5$ mM. Initial TiO_2 (Aldrich) load = 200 mg/l. pH = 2.0.

\diamond Cu(II), \bullet BA, \blacksquare BHA, \blacktriangle BAC.

Fig. 10: BHA selectivities during the three cycles: $[BA]_0 = 1.5$ mM. $[Cu(II)]_0 = 0.5$ mM. Initial TiO_2 (Aldrich) load = 200 mg/l. pH = 2.0. \circ 1th cycle, \square 2nd cycle, \triangle 3rd cycle.

Fig. 11: XPS spectra for the solid sample after the photocatalytic oxidation run.



- Use of the $\text{TiO}_2/\text{Cu(II)}$ photocatalytic system in solar pilot plant
- Selective oxidation of benzyl alcohol to the corresponding aldehyde
- Partial conversion of aldehyde to the corresponding benzoic acid
- Copper regeneration
- Evaluation of figure of merit